

Tidal Locking of Habitable Exoplanets

Rory Barnes

the date of receipt and acceptance should be inserted later

Abstract Potentially habitable planets can orbit close enough to their host star that the differential gravity across their diameters can produce an elongated shape. Frictional forces inside the planet prevent the bulges from aligning perfectly with the host star and result in torques that alter the planet's rotational angular momentum. Eventually the tidal torques fix the rotation rate at a specific frequency, a process called tidal locking. Tidally locked planets on circular orbits will rotate synchronously, but those on eccentric orbits will either librate or rotate super-synchronously. Although these features of tidal theory are well-known, a systematic survey of the rotational evolution of potentially habitable exoplanets using classic equilibrium tide theories has not been undertaken. I calculate how habitable planets evolve under two commonly-used models and find, for example, that one model predicts that the Earth's rotation rate would have synchronized after 4.5 Gyr if its initial rotation period was 3 days, it had no satellites, and it always maintained the modern Earth's tidal properties. Lower mass stellar hosts will induce stronger tidal effects on potentially habitable planets, and tidal locking is possible for most planets in the habitable zones of GKM dwarf stars. For fast rotating planets, both models predict eccentricity growth and that circularization can only occur once the rotational frequency is similar to the orbital frequency. The orbits of potentially habitable planets of very late M dwarfs ($\lesssim 0.1 M_{\odot}$) are very likely to be circularized within 1 Gyr and hence those planets will be synchronous rotators. Proxima b is almost assuredly tidally locked, but its orbit may not have circularized yet, so the planet could be rotating super-synchronously today. The evolution of the isolated and potentially habitable *Kepler* planet candidates is computed and about half could be tidally locked. Finally, projected *TESS* planets are simulated over a wide range of assumptions, and the vast majority of all cases are found to tidally lock within 1 Gyr. These results suggest that the process of tidal locking is a major factor in the evolution of most of the potentially habitable exoplanets to be discovered in the near future.

Astronomy Department, University of Washington, Box 951580, Seattle, WA 98195 · NASA Astrobiology Institute – Virtual Planetary Laboratory Lead Team, USA

1 Introduction

The role of planetary rotation on habitability has been considered for well over a century. By the late 1800’s astronomers were keenly interested in the possibility that Venus could support life, but (erroneous) observations of synchronous rotation led to considerable discussion of its impact on planetary habitability (Schiaparelli 1891; Lowell 1897; Slipher 1903; See 1910; Webster 1927). Some researchers asked “[w]ill tidal friction at the last put a stop to the sure and steady clockwork of rotation, and reduce one hemisphere to a desert, jeopardizing or annihilating all existence [of life on Venus]?” (Mumford 1909), while other, more optimistic, scientists suggested “that between the two separate regions of perpetual night and day there must lie a wide zone of subdued rose-flushed twilight, where the climatic conditions may be well suited to the existence of a race of intelligent beings” (Heward 1903). We now know that Venus is covered with thick clouds and that astronomers misinterpreted their results, but their speculations on the habitability of tidally locked worlds are similar to modern discussions.

The possibility that the rotational period of some habitable exoplanets may be modified by tidal interaction with their host stars was first suggested by Stephen Dole in his classic book *Habitable Planets for Man* over 50 years ago (Dole 1964). At the time, no exoplanets were known, but Dole, motivated by the dawning of the “space age,” was interested in the possibility that humanity could someday travel to distant star systems. Dole (1964) did not compute planetary spin evolution, but instead calculated the heights of tidal bulges in the Solar System to identify a critical height that separates synchronously and freely rotating worlds. Citing the models of Webster (1925), he settled on $\sqrt{2}$ feet (= 42 cm), and then calculated the orbital distances from a range of stellar hosts for which Earth’s tide reached that height. Assuming (somewhat arbitrarily) an “ecosphere” of our Solar System to lie between 0.725 and 1.24 AU, he concluded that all potentially habitable planets orbiting stars less than 72% the mass of the Sun would rotate synchronously and that the inner edge of the ecosphere could be affected up to 88%. As Dole believed it was “evident that low rates of rotation are incompatible with human habitability requirements,” a sense of pessimism developed regarding the possibility that planets orbiting M dwarfs could support life.

Kasting et al. (1993) returned to the problem and computed explicitly the orbital radius at which a planet similar to Earth would become a synchronous rotator around main sequence stars. In particular they used a model in which the phase lag between the passage of the perturber and the tidal bulge is constant and concluded that an Earth-like planet’s rotational frequency would synchronize with the orbital frequency in the habitable zone (HZ; the shell around a star for which runaway atmospheric feedbacks do not preclude surface water) for stellar masses $M_* < 0.42 M_\odot$ within 4.5 Gyr. They called the orbital distance at which this state developed the “tidal lock radius.” They relied on the model of Peale (1977) and used a relatively low energy dissipation rate for Earth, as suggested by models of the evolution of the Earth-Moon system in isolation (MacDonald 1964), see also § 2.4. Furthermore, Kasting et al. (1993) used a sophisticated one-dimensional photochemical-climate model to compute the HZ, which is more realistic than Dole’s ecosphere.

The study of Kasting et al. (1993) differs from Dole (1964) in that the former was interested in planets which could support liquid surface water, whereas the latter imagined where modern humans would feel comfortable. It is important to bear in mind that synchronous rotation represents a state for which the atmospheric modeling

approach of Kasting et al. (1993) breaks down – a planet with a permanent dayside and permanent nightside is not well-represented by a one-dimensional model in altitude – not a fundamental limit to the stability of surface water on an Earth-like planet. Nonetheless, Kasting et al. (1993) retained Dole’s pessimism and concluded that “all things considered, M stars rank well below G and K stars in their potential for harboring habitable planets.” Clearly the meaning of “habitable” is important in this discussion, and has affected how scientists interpret their results in terms of the search for life-bearing worlds. In this study, a “habitable planet” is one that is mostly rock with liquid water oceans (that may be global) and a relatively thin ($\lesssim 1000$ bars) atmosphere.

With the development of 3-dimensional global climate models (GCMs), the surface properties of synchronously rotating planets can be explored more self-consistently. The first models were relatively simple, but found that synchronously rotating planets can support liquid water and hence should be considered potentially habitable (Joshi et al. 1997). More recent investigations have confirmed this result (Wordsworth et al. 2011; Pierrehumbert 2011; Yang et al. 2013; Way et al. 2015; Shields et al. 2016; Kopparapu et al. 2016), and hence we should no longer view synchronous rotation as a limit to planetary habitability. Moreover, these GCM models suggest the HZ for synchronous rotators may extend significantly closer to the host star than 1-D models predict (Yang et al. 2013). These are precisely the planets likely to be discovered by the upcoming Transiting Exoplanet Survey Satellite (*TESS*) mission (Ricker et al. 2014; Sullivan et al. 2015), and may also be amenable to transit transmission spectroscopy by the *James Webb Space Telescope*. Furthermore, low-mass stars are more common than Sun-like stars and so a significant number of exoplanets in the HZ of nearby stars may be in a synchronous state and with a rotational axis nearly parallel with the orbital axis (Heller et al. 2011).

Some recent studies have examined the rotational evolution of planets and satellites (Ferraz-Mello 2015; Makarov 2015), but did not consider their results in relation to the HZ. Motivated by the potential to detect extraterrestrial life, I have performed a systematic study of the tidal evolution of habitable planets to provide more insight into the physical and orbital properties that can lead to significant rotational evolution and in some cases synchronous rotation. This survey focuses solely on the two-body problem and neglects the role of companions and spin-orbit resonances, both of which could significantly affect the tidal evolution, *e.g.* (Wu and Goldreich 2002; Mardling and Lin 2002; Rodríguez et al. 2012; Van Laerhoven et al. 2014). In particular, I will use the “equilibrium tide” (ET) model, first proposed by Darwin (1880) and described in more detail in § 2, to simulate the orbital and rotational evolution of rocky planets with masses between 0.1 and 10 M_{\oplus} orbiting stars with masses between 0.07 and 1.5 M_{\odot} for up to 15 Gyr.

Kasting et al. (1993) employed an ET model and made many assumptions and approximations, but it was vastly superior to the method of Dole. The Kasting et al. model used a 1 M_{\oplus} , 1 R_{\oplus} planet with zero eccentricity, no companions, no obliquity, and an initial rotation period of 13.5 hours to compute the orbital radius at which tidal effects cause the planet to become a synchronous rotator. In the ET model of Peale (1977), the rate of tidal evolution scales linearly with the so-called “tidal quality factor” Q , which essentially links energy dissipation by friction with the torques due to asymmetries in the bodies. Kasting et al. (1993) chose $Q = 100$ as suggested by MacDonald (1964) despite the fact that modern measurements based on lunar laser ranging, see Dickey et al. (1994), find that Earth’s value is 12 ± 2 (Williams et al. 1978). Kasting et al. (1993) also ignored the ET models’ predictions that large eccentricities ($e \gtrsim 0.1$) could result in supersynchronous rotation (Goldreich 1966; Barnes et al. 2008; Ferraz-Mello et al.

2008; Correia et al. 2008). ET models are not well-calibrated at large eccentricities, but given the large number of large exoplanets with large eccentricities, it may be that many planets are “tidally locked,” meaning their rotation rate is fixed by tidal torques, yet they do not rotate synchronously.

The method of calculating HZ boundaries of Kasting et al. (1993) has been improved several times, *e.g.* (Selsis et al. 2007; Kopparapu et al. 2013), and these studies typically include a curve that is similar to that in Kasting et al. (1993) which indicates that rotational synchronization is confined to the M spectral class. Such a sharp boundary in tidal effects is misleading, as the initial conditions of the rotational and orbital properties can span orders of magnitude, the tidal dissipation rate is poorly constrained, and the tidal models themselves are poor approximations to the physics of the deformations of planetary surfaces, particularly those with oceans and continents. We should expect a wide range of spin states for planets in the HZ of a given stellar mass, an expectation that is borne out by the simulations presented below in § 3.

The ET model ignores many phenomena that may also affect a planet’s rotational evolution such as atmospheric tides (Gold and Soter 1969; Correia and Laskar 2001, 2003; Leconte et al. 2015), the influence of companions, *e.g.* (Correia et al. 2013; Greenberg et al. 2013), rotational braking by stellar winds (Matsumura et al. 2010; Reiners et al. 2014), etc. These effects can be significant, perhaps even dominant, and recently some researchers have improved on ET models by including more realistic assumptions about planetary and stellar interiors, *e.g.* (Henning et al. 2009; Correia 2006; Ferraz-Mello 2013; Zahnle et al. 2015; Driscoll and Barnes 2015). However, tidal dissipation on Earth occurs primarily in the oceans as a result of nonlinear processes and is not well-approximated by assumptions of homogeneity. Satellite data reveal that about two-thirds of Earth’s dissipation occurs in straits and shallow seas and about one-third in the open ocean (Egbert and Ray 2000). The former represent bottlenecks in flow as the tidal bulge passes and turbulence leads to energy dissipation. The latter is probably due to seafloor topography in which gravity waves are generated by ocean currents passing over undersea mountain ranges, leading to non-linear wave interactions that cause energy dissipation. Thus, the tidal braking of an Earth-like planet is most dependent on the the unknown properties of a putative ocean. As no “exo-oceanography” model has been developed, the ET models seem reasonable choices to explore the timescales for tidal braking of habitable exoplanets, but with the caveat that they are not accurate enough to draw robust conclusions in individual cases, rather they should only be used to identify the range of possible behavior. Also note that an implication of Egbert and Ray (2000)’s result is that exoplanets covered completely by liquid water will likely only be a few times less dissipative than one with a dichotomous surface like Earth.

This study focuses on the behavior predicted by the ET model over a wide range of initial conditions using two popular incarnations. Consideration of this broader range of parameter space reveals that nearly any potentially habitable planet could have its rotation period affected by tides. About half of *Kepler*’s isolated planet candidates are tidally locked if they possess Earth’s tidal properties, and Proxima b is found to have a tidal locking time of less than 10^6 years for all plausible assumptions. I also calculate the time to tidally lock, T_{lock} for the projected yields of NASA’s upcoming *TESS* mission and find that in almost all cases $T_{lock} < 1$ Gyr, suggesting all potentially habitable worlds it detects will have had their rotations modified significantly by tidal processes. I also examine how eccentricity can grow in some cases in which a habitable planet is rotating super-synchronously, a process that has been briefly discussed

for non-habitable worlds (Heller et al. 2010; Cheng et al. 2014). In most cases, eccentricity growth is modest, and primarily acts to delay circularization. In § 4 I discuss these results in terms of exoplanet observations in general, and the possible impact on planetary habitability.

2 The Equilibrium Tide Model

The ET model assumes the gravitational force of the tide-raiser produces an elongated (prolate) shape of the perturbed body and that its long axis is slightly misaligned with respect to the line that connects the two centers of mass. This misalignment is due to dissipative processes within the deformed body and leads to a secular evolution of the orbit and spin angular momenta. Furthermore, the bodies are assumed to respond to the time-varying tidal potential as though they are damped, driven harmonic oscillators, a well-studied system. As described below, this approach leads to a set of 6 coupled, non-linear differential equations, but note that the model is linear in the sense that there is no coupling between the surface waves that sum to the equilibrium shape. A substantial body of research is devoted to tidal theory, (*e.g.* Darwin 1880; Goldreich and Soter 1966; Hut 1981; Ferraz-Mello et al. 2008; Wisdom 2008; Efroimsky and Williams 2009; Leconte et al. 2010), and the reader is referred to these studies for a more complete description of the derivations and nuances of ET theory. For this investigation, I will use the models and nomenclature of (Heller et al. 2011), which are presented below.

ET models have the advantage of being semi-analytic, and hence can be used to explore parameter space quickly. They effectively reduce the physics of the tidal distortion to two parameters, which is valuable in systems for which very little compositional and structural information is known, *e.g.* exoplanets. However, they suffer from self-inconsistencies. A rotating, tidally deformed body does not in fact possess multiple rotating tidal waves that create the non-spherical equilibrium shape of a body. The properties of the tidal bulge are due to rigidity, viscosity, structure and frequencies. ET models are not much more than toy models for tidal evolution – calculations from first principles would require three dimensions and include the rheology of the interior and, for ocean-bearing worlds, a 3-dimensional model of currents, ocean floor topography and maps of continental margins. For exoplanets, such a complicated model is not available, nor is it necessarily warranted given the dearth of observational constraints.

The ET frameworks permit fundamentally different assumptions regarding the lag between the passage of the perturber and the passage of the tidal bulge. This ambiguity has produced two well-developed models that have reasonably reproduced observations in our Solar System, but which can diverge significantly when applied to configurations with different properties. One model assumes that the lag is a constant in phase and is independent of frequency. In other words, regardless of orbital and rotational frequencies, the phase between the perturber and the tidal bulge remains constant. Following Greenberg (2009) I will refer to this version as the “constant-phase-lag” or CPL model. At first glance, this model may seem to be the best choice, given the body is expected to behave like a harmonic oscillator: In order for the tidal waves to be linearly summed, the damping parameters must be independent of frequency. However, for eccentric orbits, it may not be possible for the phase lag to remain constant as the instantaneous orbital angular frequency changes in accordance with Kepler’s 2nd Law (Touma and Wisdom 1994; Efroimsky and Makarov 2013). This paradox has led numerous researchers to reject the CPL model, despite its relative success at reproducing features in the So-

lar System, *e.g.* (MacDonald 1964; Hut 1981; Goldreich and Soter 1966; Peale et al. 1979), as well as the tidal circularization of close-in exoplanets (Jackson et al. 2008).

The second possibility for the lag is that the time interval between the perturber’s passage and the tidal bulge is constant. In this case, as frequencies change, the angle between the bulge and the perturber changes. I will call this version the “constant-time-lag,” or CTL, model (Mignard 1979; Hut 1981; Greenberg 2009). The CPL and CTL models, while qualitatively different, reduce to the same set of governing equations if a linear dependence between phase lags and tidal frequencies is assumed.

In terms of planetary rotation rate, many of the timescales are set by masses, radii, and semi-major axes. For typical main sequence stars, and Mars- to Neptune-sized planets in the classic HZ of Kasting et al. (1993), the timescales range from millions to trillions of years, with the shortest timescales occurring for the largest planets orbiting closest to the smallest stars. The CPL and CTL models predict qualitatively similar behavior for the orbital evolution of close-in exoplanets when rotational effects are ignored, *e.g.* (Jackson et al. 2009; Levrard et al. 2009; Barnes et al. 2013; Barnes 2015).

The two tidal models are effectively indistinguishable in our Solar System. Most tidally-interacting pairs of worlds are now evolving so slowly that changes due to tidal evolution are rarely measurable. The Earth-Moon system is by far the best measured, but interpretations are hampered by the complexity of the binary’s orbital history and the dissipation of energy due to Earth’s ever-changing continental configuration (Green et al. 2017). Nonetheless, the present state of the Earth-Moon system provides crucial insight into the rotational evolution of habitable exoplanets.

When the ET framework is limited to two bodies, it consists of 6 independent parameters: the semi-major axis a , the eccentricity e , the two rotation rates Ω_i , and two obliquities ψ_i , where i ($=1,2$) corresponds to one of the bodies. If the gravitational gradient across a freely rotating body induces sufficient strain on that body’s interior to force movement, then frictional heating is inevitable. The energy for this heating comes at the expense of the orbit and/or rotation, and hence tidal friction decreases the semi-major axis and rotation period. The friction will also prevent the longest axis of the body to align exactly with the perturber. With an asymmetry introduced, torques arise and open pathways for angular momentum exchange. There are three reservoirs of angular momentum: the orbit and the two rotations. ET models assume orbit-averaged torques, which is a good approximation for the long-term evolution of the system. The redistribution of angular momentum depends on the amount of energy dissipated, and the heights and positions of the tidal bulges relative to the line connecting the two centers of mass. The ET model can therefore be seen as a mathematical construction that couples energy transformation to conservation of angular momentum.

The tidal power and bulge properties depend on the composition and microphysics of planetary and stellar interiors, which are very difficult to measure in our Solar System, let alone in an external planetary system. In ET theory, the coupling between energy dissipation and the tidal bulge is therefore a central feature, and are scaled by two parameters, the Love number of degree 2, k_2 , and a parameter that represents the lag between the line connecting the two centers of mass and the direction of the tidal bulge. In the CPL model, this parameter is the “tidal quality factor” Q , and in CTL it is the tidal time lag τ . k_2 is the same in both models.

Although energy dissipation results in semi-major axis decay, angular momentum exchange can lead to semi-major axis growth. This growth can occur if enough rota-

tional angular momentum can be transferred to the semi-major axis to overcome its decay due to tidal heating. Earth and the Moon are in this configuration now.

A tidally evolving system has three possible final configurations (Counselman 1973): both bodies rotate synchronously with spin axes parallel to the orbital axis and they revolve around each other on a circular orbit; the two bodies merge; or the orbit expands forever. The first case is called “double synchronous rotation”, and is the only stable solution. In the latter case, encounters with other massive bodies will likely prevent the unimpeded expansion of the orbit. As the rotation rates decay, the less massive body will probably be the first to reach the synchronous state, and this is the case for habitable exoplanets of main sequence stars.

2.1 The Constant Phase Lag Model

In the 2nd order CPL model of tidal evolution, the angle between the line connecting the centers of mass and the tidal bulge is constant. This approach is commonly utilized in Solar System studies (*e.g.* Goldreich and Soter 1966; Greenberg 2009) and the evolution is described by the following equations:

$$\frac{de}{dt} = -\frac{ae}{8GM_1M_2} \sum_{i=1}^2 Z'_i \left(2\varepsilon_{0,i} - \frac{49}{2}\varepsilon_{1,i} + \frac{1}{2}\varepsilon_{2,i} + 3\varepsilon_{5,i} \right), \quad (1)$$

$$\frac{da}{dt} = \frac{a^2}{4GM_1M_2} \sum_{i=1}^2 Z'_i \left(4\varepsilon_{0,i} + e^2 \left[-20\varepsilon_{0,i} + \frac{147}{2}\varepsilon_{1,i} + \frac{1}{2}\varepsilon_{2,i} - 3\varepsilon_{5,i} \right] - 4 \sin^2(\psi_i) \left[\varepsilon_{0,i} - \varepsilon_{8,i} \right] \right),$$

$$\frac{d\Omega_i}{dt} = -\frac{Z'_i}{8M_i r_{g,i}^2 R_i^2 n} \left(4\varepsilon_{0,i} + e^2 \left[-20\varepsilon_{0,i} + 49\varepsilon_{1,i} + \varepsilon_{2,i} \right] + 2 \sin^2(\psi_i) \left[-2\varepsilon_{0,i} + \varepsilon_{8,i} + \varepsilon_{9,i} \right] \right),$$

and

$$\frac{d\psi_i}{dt} = \frac{Z'_i \sin(\psi_i)}{4M_i r_{g,i}^2 R_i^2 n \Omega_i} \left(\left[1 - \xi_i \right] \varepsilon_{0,i} + \left[1 + \xi_i \right] \left\{ \varepsilon_{8,i} - \varepsilon_{9,i} \right\} \right), \quad (2)$$

where t is time, G is Newton’s gravitational constant, M_i are the two masses, R_i are the two radii, and n is the mean motion. The above equations are mean variations of the orbital elements, averaged over the orbital the period, and are only valid to second order in e and ψ . The quantity Z'_i is

$$Z'_i \equiv 3G^2 k_{2,i} M_j^2 (M_i + M_j) \frac{R_i^5}{a^9} \frac{1}{nQ_i}, \quad (3)$$

where $k_{2,i}$ are the Love numbers of order 2, and Q_i are the “tidal quality factors.” The parameter ξ_i is

$$\xi_i \equiv \frac{r_{g,i}^2 R_i^2 \Omega_i a n}{GM_j}, \quad (4)$$

where i and j refer to the two bodies, and r_g is the “radius of gyration,” *i.e.* the moment of inertia is $M(r_g R)^2$. The signs of the phase lags are

$$\begin{aligned}
\varepsilon_{0,i} &= \Sigma(2\Omega_i - 2n) \\
\varepsilon_{1,i} &= \Sigma(2\Omega_i - 3n) \\
\varepsilon_{2,i} &= \Sigma(2\Omega_i - n) \\
\varepsilon_{5,i} &= \Sigma(n) \\
\varepsilon_{8,i} &= \Sigma(\Omega_i - 2n) \\
\varepsilon_{9,i} &= \Sigma(\Omega_i) ,
\end{aligned} \tag{5}$$

with $\Sigma(x)$ the sign of any physical quantity x , *i.e.* $\Sigma(x) = +1, -1$ or 0 .

The CPL model described above only permits 4 “tidal waves”, and hence does not allow this continuum, only spin to orbit frequency ratios of 3:2 and 1:1. Essentially, for eccentricities below $\sqrt{1/19}$, the torque on the rotation by the tidal waves is insufficient to change the rotation rate, but above it, the torque is only strong enough to increase the rotation rate to $1.5n$. In other words, these rotation rates are the only two resolved by the truncated infinite series used in the CPL framework, and the equilibrium rotation period is

$$P_{eq}^{CPL} = \begin{cases} P, & e < \sqrt{1/19} \\ \frac{2P}{3}, & e \leq \sqrt{1/19}, \end{cases} \tag{6}$$

where P is the orbital period. (Goldreich 1966) suggested that the equilibrium rotation period, *i.e.* the rotation period of a “tidally locked” body, is

$$P_{eq}^{G66} = \frac{P}{1 + 9.5e^2}. \tag{7}$$

(Murray and Dermott 1999) presented a derivation of this expression, which assumes $\sin(\psi) = 0$, and predicts the rotation rate may take a continuum of values.

Barnes et al. (2013) suggested the CPL model should be implemented differently depending on the problem. When modeling the evolution of a system, one should use the discrete spin values for self-consistency, *i.e.* as an initial condition, or if forcing the spin to remain tide-locked. However, if calculating the equilibrium spin period separately, the continuous value of Eq. (6) should be used. I refer to these rotational states as “discrete” and “continuous” and will use the former throughout this study.

Note in Eq. (1) that e can grow if

$$\sum_{i=1}^2 Z_i \left(2\varepsilon_{0,i} - \frac{49}{2}\varepsilon_{1,i} + \frac{1}{2}\varepsilon_{2,i} + 3\varepsilon_{5,i} \right) < 0, \tag{8}$$

which depends on the orbital and rotational frequencies, as well as the physical properties of the two bodies. Eccentricity growth by tidal effects has been considered for brown dwarfs (Heller et al. 2010), but has not been examined for potentially habitable exoplanets. If e grows, then by Eq. (6), we expect a planet’s equilibrium rotational period to decrease, *i.e.* it will never be synchronized. Thus, synchronization is not necessarily the end state of the tidal evolution of a planet’s spin, if the equilibrium tide models are approximately valid at high eccentricity.

2.2 The Constant Time Lag Model

The CTL model assumes that the time interval between the passage of the perturber and the tidal bulge is constant. This assumption allows the tidal response to be continuous over a wide range of frequencies, unlike the CPL model. But, if the phase lag is a function of the forcing frequency, then the system is no longer analogous to a damped driven harmonic oscillator. Therefore, this model should only be used over a narrow range of frequencies, see (Greenberg 2009). However, this model's use is widespread, especially at high e , so I use it to evaluate tidal effects as well.

Here I use the model derived by (Leconte et al. 2010), with the nomenclature of Heller et al. (2011). The evolution is described by the following equations:

$$\frac{de}{dt} = \frac{11ae}{2GM_1M_2} \sum_{i=1}^2 Z_i \left(\cos(\psi_i) \frac{f_4(e)}{\beta^{10}(e)} \frac{\Omega_i}{n} - \frac{18}{11} \frac{f_3(e)}{\beta^{13}(e)} \right), \quad (9)$$

$$\frac{da}{dt} = \frac{2a^2}{GM_1M_2} \sum_{i=1}^2 Z_i \left(\cos(\psi_i) \frac{f_2(e)}{\beta^{12}(e)} \frac{\Omega_i}{n} - \frac{f_1(e)}{\beta^{15}(e)} \right), \quad (10)$$

$$\frac{d\Omega_i}{dt} = \frac{Z_i}{2M_i r_{g,i}^2 R_i^2 n} \left(2 \cos(\psi_i) \frac{f_2(e)}{\beta^{12}(e)} - \left[1 + \cos^2(\psi) \right] \frac{f_5(e)}{\beta^9(e)} \frac{\Omega_i}{n} \right), \quad (11)$$

and

$$\frac{d\psi_i}{dt} = \frac{Z_i \sin(\psi_i)}{2M_i r_{g,i}^2 R_i^2 n \Omega_i} \left(\left[\cos(\psi_i) - \frac{\xi_i}{\beta} \right] \frac{f_5(e)}{\beta^9(e)} \frac{\Omega_i}{n} - 2 \frac{f_2(e)}{\beta^{12}(e)} \right). \quad (12)$$

where

$$Z_i \equiv 3G^2 k_{2,i} M_j^2 (M_i + M_j) \frac{R_i^5}{a^9} \tau_i, \quad (13)$$

and

$$\begin{aligned} \beta(e) &= \sqrt{1 - e^2}, \\ f_1(e) &= 1 + \frac{31}{2}e^2 + \frac{255}{8}e^4 + \frac{185}{16}e^6 + \frac{25}{64}e^8, \\ f_2(e) &= 1 + \frac{15}{2}e^2 + \frac{45}{8}e^4 + \frac{5}{16}e^6, \\ f_3(e) &= 1 + \frac{15}{4}e^2 + \frac{15}{8}e^4 + \frac{5}{64}e^6, \\ f_4(e) &= 1 + \frac{3}{2}e^2 + \frac{1}{8}e^4, \\ f_5(e) &= 1 + 3e^2 + \frac{3}{8}e^4. \end{aligned} \quad (14)$$

It can also be shown that the equilibrium rotation period is

$$P_{eq}^{CTL}(e, \psi) = P \frac{\beta^3 f_5(e) (1 + \cos^2 \psi)}{2f_2(e) \cos \psi}, \quad (15)$$

which for low e and $\psi = 0$ reduces to

$$P_{eq}^{CTL} = \frac{P}{1 + 6e^2}. \quad (16)$$

Fig. 1 shows the predicted ratio of the equilibrium rotational frequency Ω_{eq} to n as a function of e for the CPL model (solid curve), Goldreich (1966)'s model (dotted) and the CTL model (dashed). All models predict that as e increases, the rotational

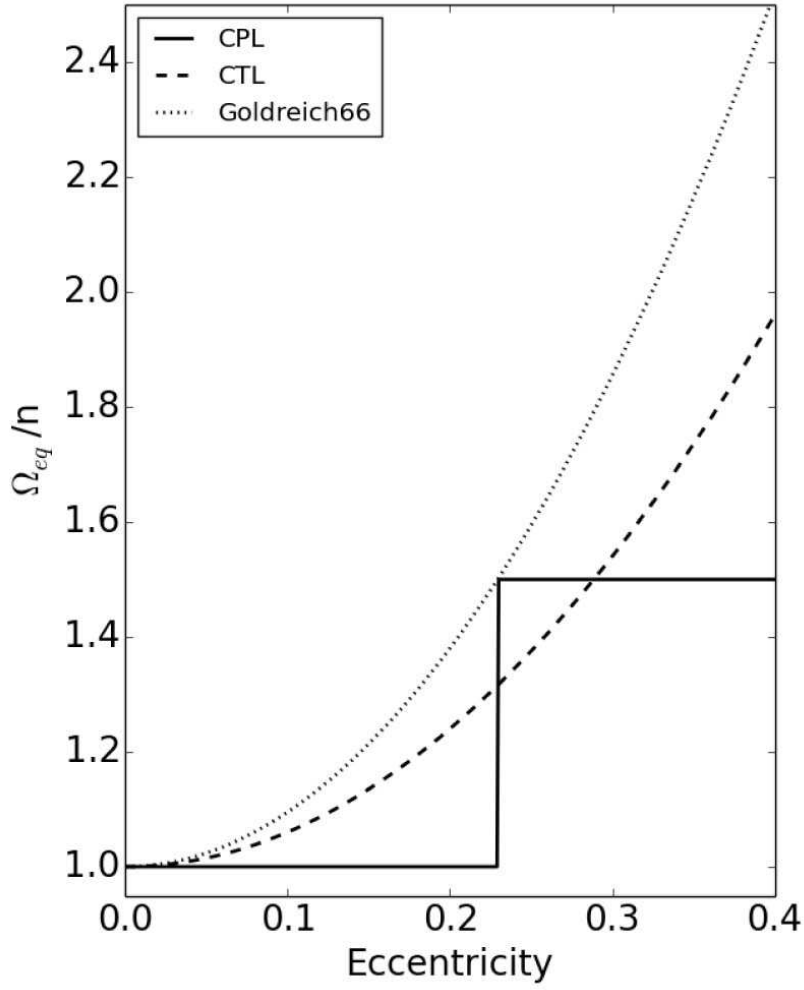


Fig. 1 Equilibrium spin frequency of a tidally locked exoplanet as a function of eccentricity for the CPL model (solid curve), the CTL model (dashed), and Goldreich (1966)'s model (dotted).

frequency of a tidally locked planet will grow, and hence planets found on eccentric orbits may rotate super-synchronously.

As in the CPL model, the CTL model also predicts configurations that lead to eccentricity growth, which could prevent rotational synchronization. If

$$\sum_{i=1}^2 Z_i \left(\cos(\psi_i) \frac{f_4(e)}{\beta^{10}(e)} \frac{\Omega_i}{n} - \frac{18}{11} \frac{f_3(e)}{\beta^{13}(e)} \right) > 0 \quad (17)$$

then the orbital eccentricity will grow.

2.3 Numerical Methods (EQTIDE)

To survey the range of rotational evolution of habitable exoplanets, I performed thousands of numerical simulations of individual star-planet pairs and tracked their orbital and rotational states. To compute the models described in the previous two subsections I used the software package `EQTIDE`¹. This code, written in C, is fast, user-friendly, and has a simple switch between the CTL and CPL models. The governing equations are calculated with a 4th order Runge-Kutta integrator (although Euler’s method works surprisingly well), with an adaptive timestep determined by the most rapidly evolving parameter. This software package and its variants have been used on a wide range of binary systems, including exoplanets (Barnes et al. 2013; Barnes 2015), binary stars (Gómez Maqueo Chew et al. 2012, 2014), brown dwarfs (Fleming et al. 2012; Ma et al. 2013), and exomoons (Heller and Barnes 2013).

For the simulations presented below, I used the Runge-Kutta method with a timestep that was 1% of the shortest dynamical time ($x/(dx/dt)$, where x is one of the 6 independent variables), and assumed a planet became tidally locked if its rotation period reached 1% of the equilibrium rotation period. If a planet becomes tidally locked, its rotation period is forced to equal the equilibrium period (Eq. [6] or Eq. [16]) for the remainder of the integration. Note that the obliquity, eccentricity and mean motion can continue to evolve and so the spin period can also.

2.4 What is the Tidal Response?

The ET models described above have two free parameters: k_2 and either Q or τ . The former can only have values between 0 and 1.5, but the latter can span orders of magnitude. As is well known, the current estimates for Q and τ of Earth, 12 and 640 s, respectively, predict that the Moon has only been in orbit for 1–2 Gyr (MacDonald 1964; Touma and Wisdom 1994), far less than its actual age of 4.5 Gyr. This contradiction has led many researchers to assume that the historical averages of Earth’s tidal Q and τ have been about 10 times different. Indeed, Kasting et al. (1993) assumed $Q = 100$ when they calculated their tidal lock radius. Previous researchers have argued that such discrepancies are justified because tidal dissipation in the oceans is a complex function of continental positions and in the past different arrangements could have allowed for weaker dissipation. A recent study of ocean dissipation over the past 250 Myr found that the modern Earth is about twice as dissipative as compared to the historical average (Green et al. 2017). Another possibility is that the continents grow with time (Dhuime et al. 2012) resulting in a larger fraction of the surface consisting of highly dissipative straits and shallow seas. Whether these suppositions are true remains to be seen, but clearly the ET models fail when using modern values of the tidal dissipation. On the other hand, if Q (τ) has been shrinking (growing) then we might expect it to continue to do so, and planets older than Earth may be more dissipative.

However, one also needs to bear in mind the complexities of the Earth-Moon system’s presence in the Solar System. Čuk (2007) showed that the Moon’s orbit and obliquity have been perturbed by passages through secular resonances with Venus and Jupiter as the Moon’s orbit expanded. During these perturbations, the eccentricity of the Moon could have reached 0.2 and hence the simple picture invoked by classic

¹ Publicly available at <https://github.com/RoryBarnes/EqTide>.

studies of the two-body Earth-Moon system may be invalid (and that there may have been epochs in Earth history during which the Moon rotated super-synchronously). Moreover, the early evolution of the Earth-Moon system may have been affected by an evection resonance involving the Earth’s orbit about the Sun and by energy dissipation inside the solid Earth (Ćuk and Stewart 2012; Zahnle et al. 2015). Given these complications, it is unclear that the modern dissipation of Earth is not representative of its historical average, nor is it obvious that other ocean-bearing exoplanets should tend to have less dissipation than Earth.

In Fig. 2 the semi-major axis and eccentricity history of the Earth-Moon system is shown for the two ET models with different choices for the tidal response and different approximations. For the simple case of a circular orbit and no obliquities, I recover the classic results. However, dissipation rates that are 10 times less than the current rate, as advocated by Kasting et al. (1993), do not accurately calibrate the models either. Instead I find rates that are 3–5 times weaker place the Moon at Earth’s surface 4.5 Gyr ago ($Q = 34.5$ and $\tau = 125$ s). When the assumption that $e = \sin \psi = 0$ is relaxed and the modern values are used, the CTL model predicts slightly different behavior, but the CPL model is qualitatively different and actually predicts large values of a and e in the past. This history is strongly influenced by the current values of e and ψ , which were modified by the secular resonance crossings (Ćuk 2007).

In summary, the ET models predict reasonable histories for the Earth-Moon system, but the history is sufficiently complicated that we cannot unequivocally state that the modern Earth’s Q and τ values should be discarded when considering habitable exoplanets. It is also currently impossible to know how different continents and seafloor topography affect the tidal response of habitable exoplanets. In light of these uncertainties, I will use the modern Earth’s values of Q and τ in the simulations of the tidal evolution of habitable exoplanets. In general the timescales scale linearly with these parameters, so if one prefers different choices, it is relatively straight-forward to estimate the evolution based on the plots provided below, or to directly calculate it with EQTIDE.

2.5 Initial Conditions

Every trial run requires specific physical and orbital properties, some of which can be constrained by models, but others cannot. A star’s mass is roughly constant over its main sequence lifetime, but its radius and luminosity can change significantly over time. I fit the 5 Gyr mass-radius-luminosity relation from Baraffe et al. (2015) to a third order polynomial using Levenberg-Marquardt minimization (Press et al. 1992) and found

$$\frac{R_*}{R_\odot} = 0.003269 + 1.304 \frac{M_*}{M_\odot} - 1.312 \frac{M_*^2}{M_\odot} + 1.055 \frac{M_*^3}{M_\odot}, \quad (18)$$

and

$$\log \left(\frac{L_*}{L_\odot} \right) = -0.0494 + 6.65X + 8.73X^2 + 5.208X^3, \quad (19)$$

where $X = \log(M_*/M_\odot)$. The star’s k_2 , Q , and τ values are set to 0.5, 10^6 , and 0.01 s for all cases, similar to previous studies (Rasio et al. 1996; Jackson et al. 2008; Matsumura et al. 2010; Barnes 2015). For the CPL model, the initial values of the phase lags are determined by the initial rotational and orbital frequencies as described in Eq. (5).

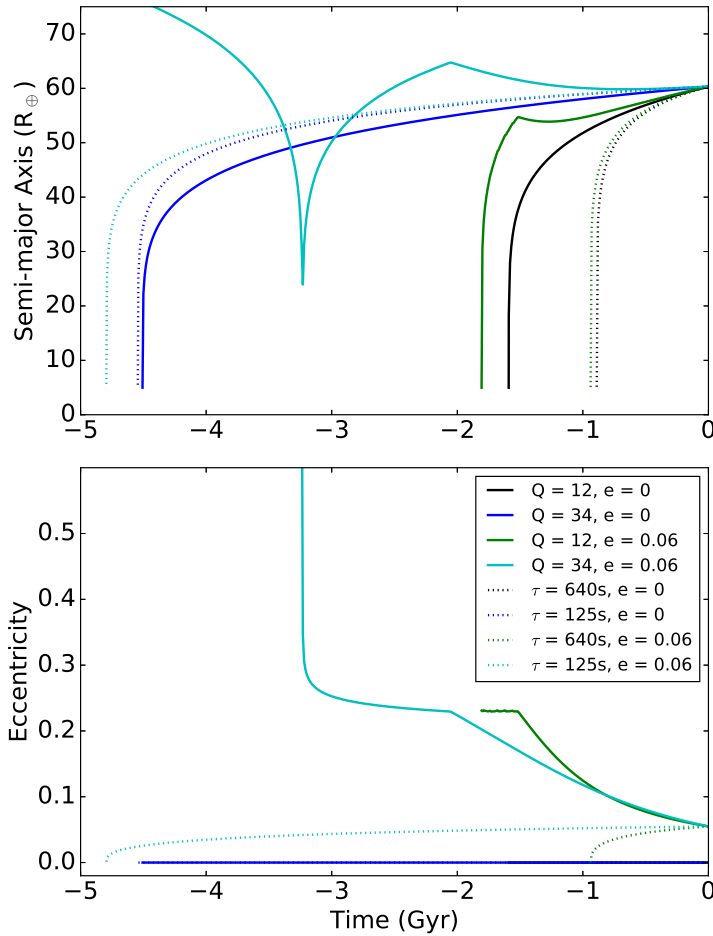


Fig. 2 Tidal evolution of the semi-major axis (top) and eccentricity (bottom) of the Earth-Moon system for different assumptions. Solid curves correspond to the CPL model, dotted to CTL. The black curves assume the modern value of Earth’s tidal response, but the eccentricity and 2 obliquities have been set to 0. These curves reproduce the classic result that the Moon was at Earth’s surface 1–2 Gyr ago. The blue curves show the history if the Q and τ values are chosen so that the Moon’s orbit began expanding 4.5 Gyr ago. The green curves use the modern tidal response and the current values of e and ψ . Cyan curves are similar, but use the calibrated values of Q and τ .

For the planet, I used the mass-radius relationship of Sotin et al. (2007) for planets with Earth-like composition:

$$\frac{R_p}{R_\oplus} = \begin{cases} \left(\frac{M_p}{M_\oplus}\right)^{0.306}, & 10^{-2} M_\oplus < M_p < M_\oplus \\ \left(\frac{M_p}{M_\oplus}\right)^{0.274}, & M_\oplus < M_p < 10 M_\oplus. \end{cases} \quad (20)$$

The planet’s k_2 , Q , and τ values are set to 0.3, 12 and 640 s (Lambeck 1977; Williams et al. 1978; Yoder 1995).

Fixing each of the physical parameters as described does not represent a comprehensive study of the problem, as planets and stars of a given mass can have a wide range of radii and tidal response. However, as shown in the next section, using these standard parameters and allowing the initial rotation period to vary admits a wide enough range of possibilities that there is no need to explore the other parameters at this time.

I also calculate the predicted tidal evolution of planets found by *Kepler*, and projected for *TESS*. For these simulations, I used both the CPL and CTL model, and three sets of initial conditions: $(P_0, \psi_0, Q, \tau) = (10 \text{ d}, 0, 12, 640 \text{ s})$, $(1 \text{ d}, 23.5^\circ, 34, 125 \text{ s})$, and $(8 \text{ hr}, 60^\circ, 100, 64 \text{ s})$, where P_0 is the initial rotation period. I will refer to these options as “short”, “Earth-like”, and “long” timescales for T_{lock} , respectively.

3 Results

This section considers the tidal evolution of ocean-bearing exoplanets orbiting various stars and with different, but reasonable, initial and physical conditions with the goal of mapping out regions of parameter space that lead to synchronous rotation on Gyr timescales. First, I consider the tidal evolution of Kepler-22 b, a $2.3 R_\oplus$ planet orbiting a G5V star near the inner edge of its HZ with no known companions (Borucki et al. 2012). This planet is probably too large to be terrestrial (Rogers 2015), but is similar to others worlds that may be (Dumusque et al. 2014; Espinoza et al. 2016), and so is potentially habitable (Barnes et al. 2015). Next I examine the tidal evolution of the recently-discovered planet Proxima Centauri b (Anglada-Escudé et al. 2016). Then I consider the potentially habitable planets discovered by the *Kepler* spacecraft that do not have planetary companions. Then I survey a broad range of parameter space and show that habitable exoplanets of G dwarf stars with an initially slow rotation period and low obliquity can become tidally locked within 1 Gyr. Next I explore the coupled orbital/rotational evolution of planets orbiting very small stars ($\lesssim 0.1 M_\odot$) and find that they are likely to be synchronous rotators. Finally, I compute the rotational evolution of the projected exoplanet yield from *TESS* (Sullivan et al. 2015) and find that nearly every potentially habitable planet the mission will discover will be tidally locked.

3.1 Kepler-22 b

Fig. 3 shows plausible spin period evolutions of Kepler-22 b assuming a mass of $23 M_\oplus$, an initial spin period of 1 day, and an initial obliquity of 23.5° . The mass of the host star is $0.97 M_\odot$ and the initial semi-major axis is 0.849 AU. The solid curves show results from the CPL model, dashed CTL. The different line colors represent different initial eccentricity, which is not well-constrained at this time. The age of the system is not known, but could be 10 Gyr (Borucki et al. 2012). For such an age, the CPL model predicts that the planet will have spun down into a synchronous state for $e \lesssim 0.2$ and into a 3:2 spin-orbit frequency ratio for larger values. On the other hand, the CTL model predicts significantly less evolution. This system demonstrates that the CPL model predicts that tidal braking can be important in the HZs of G and K dwarfs, not just M dwarfs as is usually assumed.

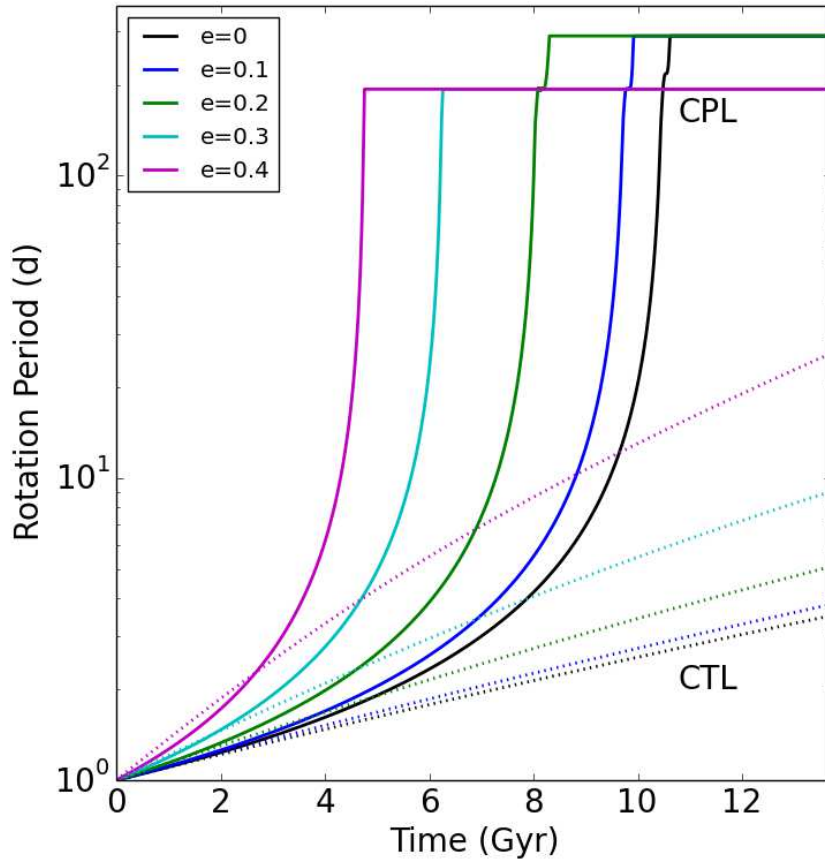


Fig. 3 Evolution of the rotation period of Kepler-22 b with different orbital eccentricities as shown in the legend. Solid lines assume the CPL model, dashed CTL. The evolution of semi-major axis and eccentricity is negligible.

3.2 Proxima Centauri b

Recently, (Anglada-Escudé et al. 2016) announced the discovery of a $\gtrsim 1.27 M_{\oplus}$ planet orbiting in the HZ of Proxima Centauri with a period of 11.2 days and an inferred semi-major axis of 0.0485 AU. The orbital eccentricity could only be constrained to be less than 0.35, and since the discovery was made via radial velocity data, the radius and actual mass are not known. Barnes et al. (2016) considered its tidal evolution in the CPL framework and found that the rotational frequency is synchronized in less than 10^6 years and that the orbital eccentricity is damped with a characteristic timescale of 1 Gyr. In this subsection I expand on those results and also consider evolution in the CTL model.

In Fig. 4 the evolution of rotation period, e and a are shown for a planet with Proxima b’s minimum mass, a radius of $1.07 R_{\oplus}$, an initial rotation period of 1 day, an initial obliquity of 23.5° , and an initial semi-major axis of 0.05 AU. The different linestyles correspond to different initial eccentricities and different tidal models.

The CPL model predicts the rotational frequency becomes locked in less than 10^4 years, and that for $e > 0.23$ planet b settles into a 3:2 spin-orbit frequency ratio that leads to semi-major axis growth. As a increases, so does the rotation period until $e \approx 0.23$ at which point the discrete nature of the CPL solution instantaneously forces the synchronous state. At this point, the torques are reversed and a begins to decrease, ultimately settling into orbits that are significantly larger than the initial orbits.

The CTL model predicts the tidal locking time to be less than 10^5 years, and that for $e > 0$ the planet will reach non-synchronous “pseudo-equilibrium” periods that are a function of e . The CTL model does not suffer from discontinuities and predicts longer times for e to damp. Thus, if Proxima b ever reached a high eccentricity state, the two ET models predict qualitatively different types of evolution.

3.3 The *Kepler* Sample

The previous examples are illustrative of the tidal evolution process for potentially habitable planets, but are not comprehensive. In this subsection, the analysis is expanded to the *Kepler* candidate planets for which no other planets are known in the system. Fig. 5 shows the time for *Kepler* candidates to tidally lock assuming they formed with 1 day rotation periods and obliquities of 23.5° . Also shown is each candidate’s “habitability index for transiting exoplanets” (HITE) (Barnes et al. 2015), which is an estimate of the likelihood that the energy received at the top of the planet’s atmosphere could permit liquid surface water and is inversely proportional to the planet’s radius, as larger planets are more likely to be gaseous and uninhabitable. For each planet candidate in Batalha et al. (2013), I calculated the tidal evolution for 6 assumptions.

The column of planets at 15 Gyr is those candidates that did not tidally lock within 15 Gyr. About half of the isolated and potentially habitable planets discovered by *Kepler* could be tidally locked. Table 1 (available in the Online Supplement) lists the properties of the planet candidates shown in Fig. 5. The previously undefined symbols are: P_{orb} = orbital period; T_{CPL}^{short} = CPL model, “short” assumptions (see § 2.5); T_{CPL}^{\oplus} = CPL model, Earth-like assumptions; T_{CPL}^{long} = CPL model, “long” assumptions; T_{CTL}^{short} = CTL model, short assumptions; T_{CTL}^{\oplus} = CTL model, Earth-like assumptions; T_{CTL}^{long} = CTL model, long assumptions.

3.4 Parameter Space Survey

Next, I consider a broader range of parameter space to explore the limits of the timescale to synchronize habitable exoplanets on circular orbits. Fig. 6 shows the results of four parameter sweeps. The left column is the CPL framework, right is CTL. The top row is the more stable case, a planet with an initial spin period of 8 hr and an initial obliquity of 60° . The bottom row shows the more unstable case, a planet with an initial spin period of 10 days, and an initial obliquity of 0° . The former has higher initial rotational angular momentum and its direction is misaligned with the orbital angular momentum, and hence it takes longer to equilibrate into the synchronous state. The

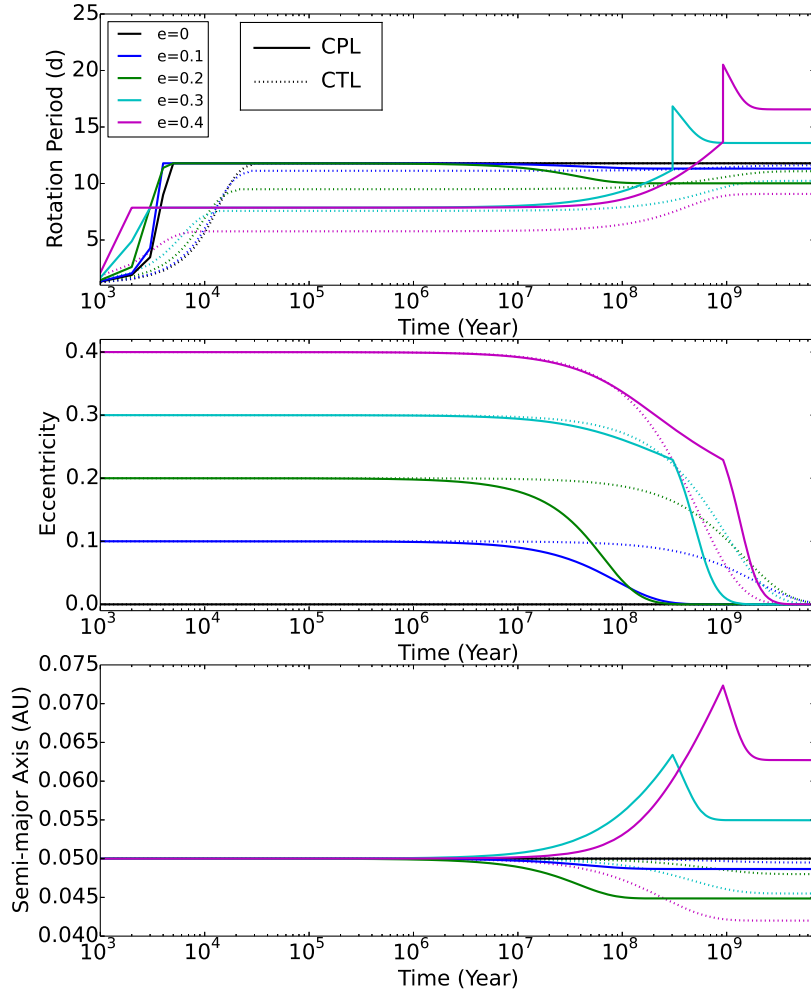


Fig. 4 Evolution of Proxima Centauri b due to tides. Solid lines assume the CPL model, dashed CTL. *Top*: Rotation period. *Middle*: Eccentricity. *Bottom*: Semi-major axis.

latter is a plausible initial condition from simulations of terrestrial planet formation (Kokubo and Ida 2007; Miguel and Brunini 2010). The HZ of Kopparapu et al. (2013) is shown as shading with the lighter gray representing empirical or optimistic limits, and the darker gray representing theoretical or conservative limits.

This figure demonstrates that for early M through G dwarfs, the possibility of rotational synchronization of habitable exoplanets on circular orbits depends on the initial conditions and the tidal response. Slower spin periods with aligned rotational and

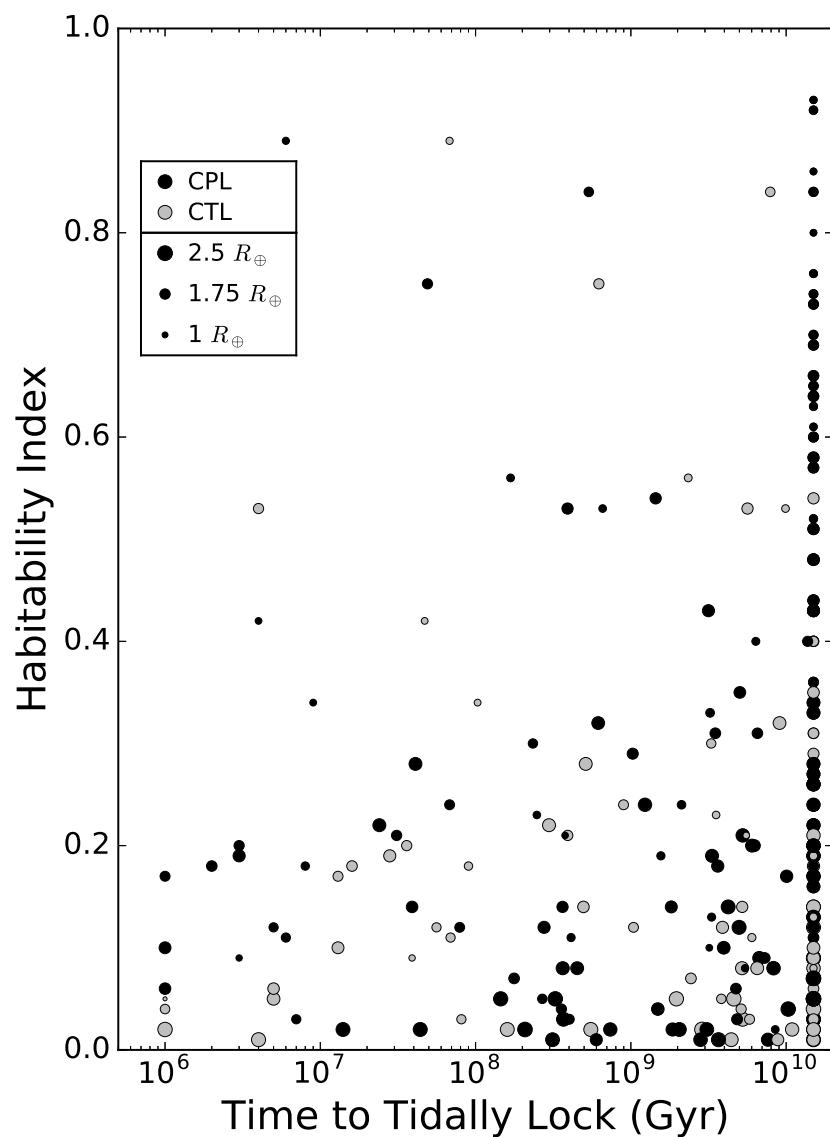


Fig. 5 Comparison of the time to tidally lock and the habitability index for transiting exoplanets. The dot size is proportional to planet mass, which is part of the habitability index, and the color corresponds to the equilibrium tide model. Planet candidates that did not tidally lock are placed at 15 Gyr.

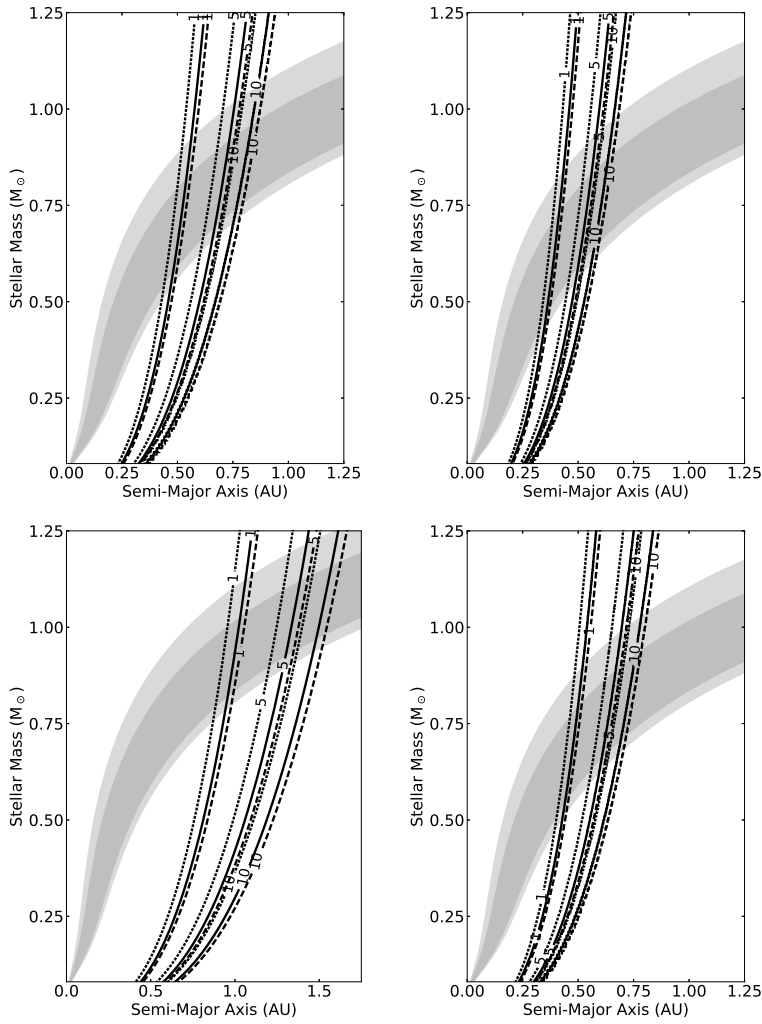


Fig. 6 Timescale for planets on circular orbits to rotate synchronously. The left panels assume the CPL model; right CTL. The top row assumes an initial rotation period of 8 hr and an obliquity of 60° . The bottom row assumes an initial rotation period of 10 days and an obliquity of 0. The HZ is shown by the gray shading, with the darker gray corresponding to the conservative HZ, and lighter grey to the optimistic HZ (Kopparapu et al. 2013). Note the different scale on the bottom left plot.

orbital axes are more likely to lead to tidal synchronization within 1 Gyr. Earth-mass planets in the HZ of the entire G spectral class can be synchronized if the CPL model is correct, but if CTL is, then planets orbiting G dwarfs will not be synchronized, unless they form with a very large rotational period, which is possible (Miguel and Brunini 2010). This difference is due to the different frequency dependencies between the two models. The ratio of Eq. (2) to Eq. (11) is $1/(2nQ\tau|n - \Omega|)$, and for an Earth with an initial rotation period of 10 days, the ratio is 9, *i.e.* the CPL model initially de-

spins the planet 9 times faster than the CTL model. The dependence on Ω forces the ratio to increase with time as $\Omega \rightarrow n$, and, indeed, for this case the difference in the time to tidally lock is a factor of 50. If Earth formed with no Moon, an initial rotation period of 3 days, and maintained a constant Q value of 12, then the CPL model predicts it would become synchronously rotating within 5 Gyr. The reader is cautioned that extrapolating from the Earth-Moon frequency to the Earth-Sun frequency could introduce significant error in the tidal modeling. The CTL's frequency dependence maintains more similar responses over a wider frequency range than CPL, and hence the CTL model does not predict such short tidal locking times for Earth-like planets in the HZ of G dwarfs.

If the assumption of a circular orbit is relaxed, then the evolution can be significantly more complicated. As demonstrated in Fig. 3, planets on higher eccentricity orbits can rotate super-synchronously. This aspect of tidal theory is well-known (Goldreich 1966; Murray and Dermott 1999; Barnes et al. 2008), but the details depend on the planet. ET models predict that super-synchronous rotation will occur for any $e > 0$, but it is far more likely that planets will be locked into spin-orbit resonance such as 1:1, 3:2, or 2:1 (Rodríguez et al. 2012). However, the tidal braking process results in transfer of rotational angular momentum to orbital angular momentum and can lead to a change in e . The sign of the change depends on the ratio of the rotational and orbital frequencies of both bodies. Previous results that predict eccentricities always decrease, such as Rasio et al. (1996) and Jackson et al. (2008), have assumed the planets had already synchronized.

The coupled evolution of the rotational frequency and the orbital eccentricity is a complex function of the dissipation rates and the distribution of the angular momentum among the spins and orbit. As can be seen in Eqs. (1) and (9), the change in eccentricity can be positive or negative depending on the ratios of several parameters. In general, e will decay for rotational periods longer than or similar to the orbital period. This behavior can be understood in terms of forces. A body rotating faster than it is revolving at pericenter will have a bulge that leads the perturber. This bulge has a gravitational force that accelerates the perturber in the direction of the motion. This acceleration increases the tangential velocity at pericenter and hence the eccentricity must grow. Because the pericenter distance must remain constant, the semi-major axis must also grow. Thus, the equilibrium rotation period can grow or shrink depending on the rates of change of a and e . As an example, the value of de/dt as a function of Ω/n for an Earth-like planet orbiting $0.1 M_{\odot}$ star with $a = 0.05$ AU and $e = 0.2$ is shown in Fig. 7. In the CPL model, planets that rotate faster than $1.5n$ will experience eccentricity growth, while slower rates lead to eccentricity decay. In the CTL model the critical frequency ratio depends on eccentricity. The difference between the two models is due to the different assumptions of the frequency dependence.

Fig. 8 shows the orbital and rotational evolution of an Earth-like planet orbiting at 0.05 AU. The eccentricity grows slightly until $n \approx 1.5\Omega$ at which point it begins to decay. For many cases, this process can act to delay the circularization process. The eccentricity distribution of radial-velocity-detected exoplanets with orbits that are unaffected by tidal interaction, *i.e.* those with $a > 0.2$ AU, has a mean² of ~ 0.3 . While the vast majority of these exoplanets is expected to be gaseous, we should nonetheless expect many terrestrial exoplanets to possess large eccentricities and those that are tidally locked will rotate super-synchronously. However e will likely also tidally

² See <http://exoplanets.org>

evolve, and hence the equilibrium period will change with time, too. As rotational evolution tends to be more rapid than orbital evolution, tidal locking generally occurs prior to orbital circularization. If $de/dt > 0$, then the planet can be tidally locked and evolving to ever shorter rotation periods. In most cases, e decays with time and hence the rotational period slows, possibly in a series of sudden transitions between spin-orbit resonances, a fascinating scenario for the biospheres of inhabited exoplanets.

Figure 9 shows the time required for the eccentricity of an Earth twin planet to drop from 0.3 to 0.01, the circularization timescale T_{circ} , for a range of stellar masses. The initial period is 1 day, and the initial obliquity is 23.5° in these calculations. The contour lines denote T_{circ} in Gyr. For both models, Earth-like planets orbiting stars less massive than $0.1 M_\odot$ will likely be on circular orbits and in synchronous rotation. Planets with initially fast rotation rates, or strong perturbations from other planets might not be synchronous rotators around stars of any mass.

3.5 TESS Projections

The results of the previous section provide a foundation to interpret future discoveries from transit (Berta-Thompson et al. 2015; Gillon et al. 2016), radial velocity (Anglada-Escudé et al. 2016), and astrometric data (Malbet et al. 2016). In the immediate future, the *Transiting Exoplanet Survey Satellite* (TESS) will likely discover dozens to hundreds of potentially habitable worlds, a handful of which could be amenable to atmospheric characterization by *JWST* (Sullivan et al. 2015; Barnes et al. 2015). In this section, I calculate the tidal evolution of the predicted sample provided by (Sullivan et al. 2015), which convolved realistic models for the detector, stellar models and variability, planet occurrence rates from *Kepler*, etc., to produce a hypothetical catalog of detected exoplanets and their properties. I find that nearly every potentially habitable planet it will discover will be tidally locked.

Fig. 10 shows the results of these simulations for the “long” cases, i.e. these represent a maximum timescale for these planets to tidally lock, assuming they are terrestrial. Nearly every planet tidally locks within 1 Gyr for both models. Table 2 lists the planets that are predicted to be single (at least in terms of those that can be discovered), and Table 3 (available in the Online Supplement) lists those planets that would be known to be in multiple planet systems. In principle, any of these predicted planets could be in a high eccentricity state, but those that are known to be in multiple systems may be more likely to have eccentricities that are sufficiently perturbed by companions to force the rotation rate into a spin-orbit resonance.

4 Discussion and Conclusions

Previous studies of the tidal evolution of habitable exoplanets identified those orbiting M dwarfs as the most likely, or perhaps only, candidates for synchronous rotation, but this study has shown that the CPL model predicts that planets orbiting in the HZ of solar-mass stars may also be synchronously rotating. Fig. 11 compares the results of Kasting et al. (1993) to the extreme contours of Fig. 6 and shows that the Kasting et al. (1993) prediction is close to the innermost “tidal lock radius” found in this study. As recent simulations of planet formation have found that initial rotation periods between 10 hours and 40 days are approximately equally likely (Miguel and Brunini 2010), the

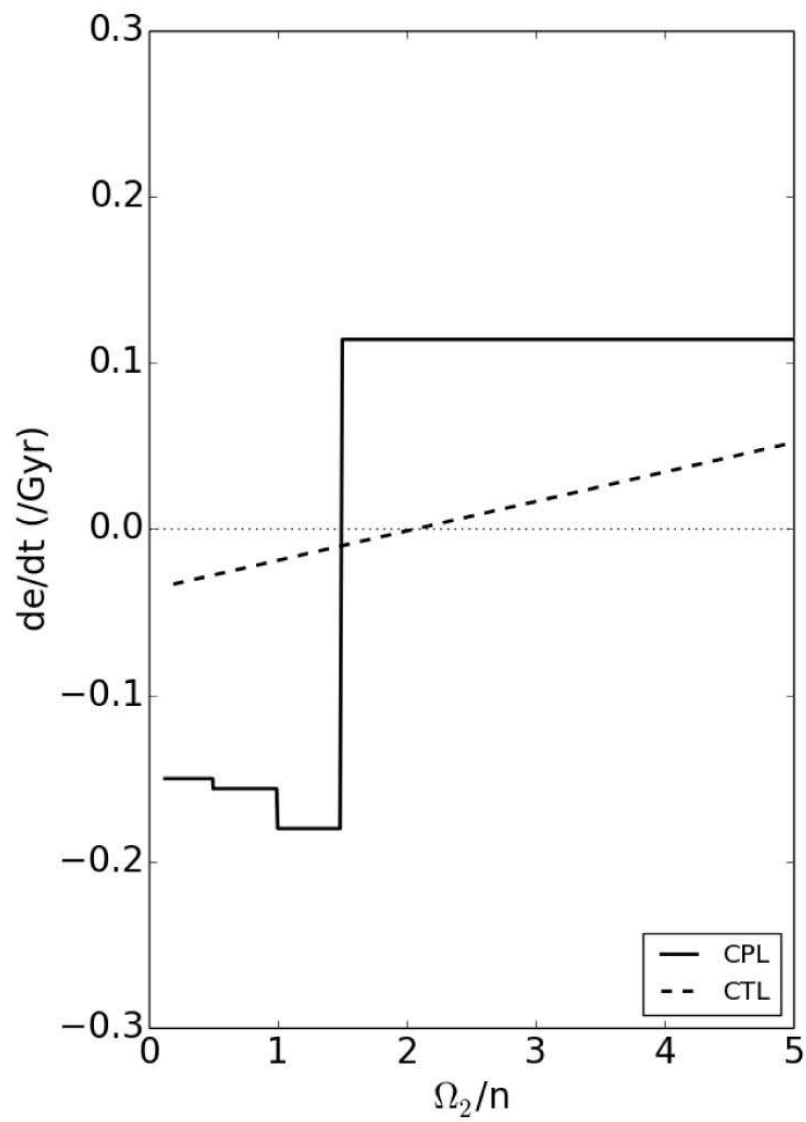


Fig. 7 de/dt for an Earth-like planet orbiting a $0.1 M_{\odot}$ star as a function of the angular frequencies, with Ω_2 being the rotational frequency of the planet. The semi-major axis of the orbit is 0.05 AU, and the eccentricity is 0.2. Both models predict that for fast rotators, de/dt is positive.

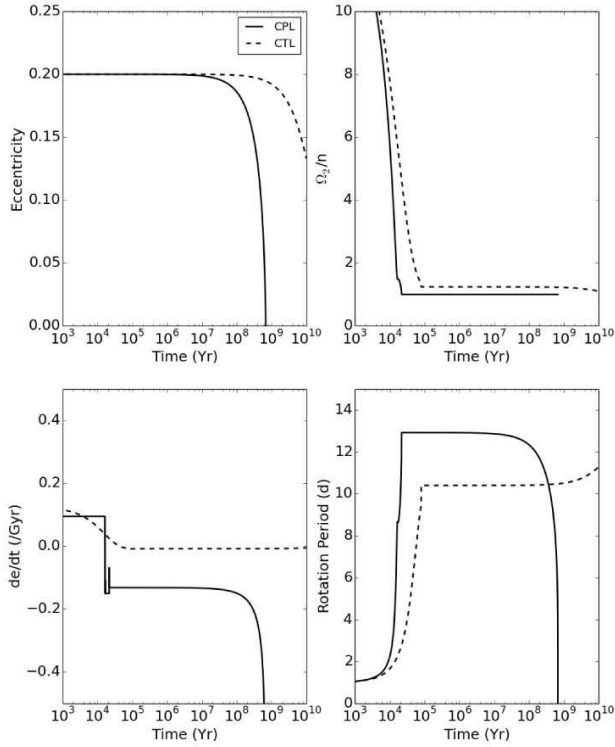


Fig. 8 Rotational and orbital evolution of an Earth-like planet orbiting a $0.1 M_{\odot}$ star at 0.05 AU. The CPL model is represented by the solid curve and the CTL by the dashed. Note that after 680 Myr the CPL model predicts the planet will merge with the host star. *Top Left:* Eccentricity. *Top Right:* The ratio of the planet’s rotational frequency to mean motion. *Bottom Left:* The time derivative of the eccentricity. The CPL predicts several discontinuities as the rotational frequency evolves. *Bottom Right:* The planet’s rotational period. The CPL model predicts a will decay rapidly after about 100 Myr, and since the planet is rotationally locked its period drops. The CTL model predicts later eccentricity damping without much evolution in a , and hence the rotational period rises.

tidal lock radius of Kasting et al. (1993) is now seen to be based on a very short initial rotation period. The above calculations only considered initial rotation periods up to 10 days, and so those results are still conservative – tidal locking may be even more likely than presented here, let alone than in Kasting et al. (1993).

As astronomers develop technologies to directly image potentially habitable planets orbiting FGK dwarfs (*e.g.* Dalcanton et al. 2015), they must be prepared for the possibility that planets orbiting any of them may be tidally locked. Such a rotation state can change planetary climate, and by extension the reflected spectra. 3D models of synchronously rotating habitable planets should be applied to planets orbiting K and G dwarfs in addition to Ms. While not explicitly considered here, habitable worlds

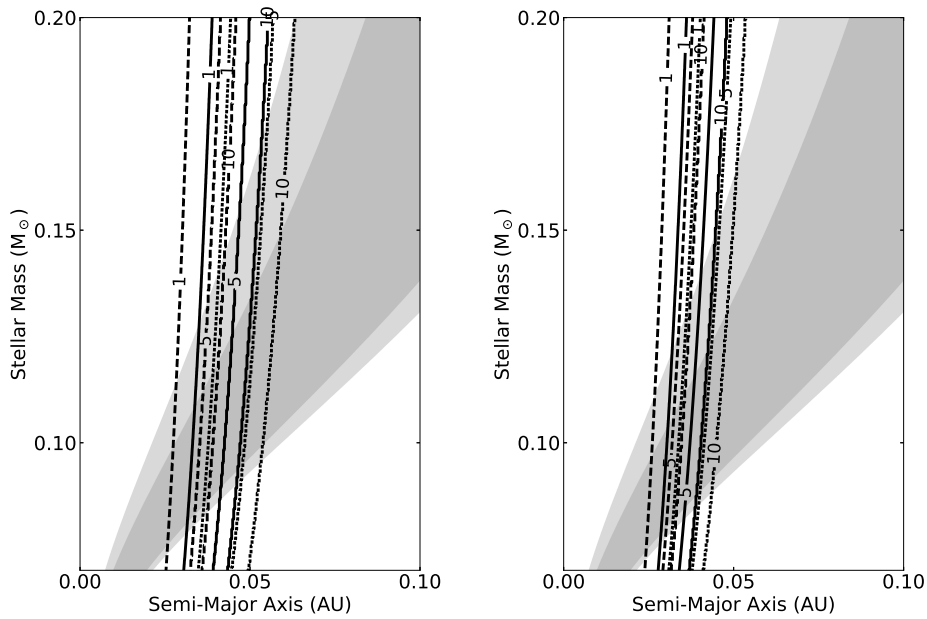


Fig. 9 The time in Gyr for an Earth-like planet with an initial eccentricity of 0.3 to circularize. The format is the same as Fig. 9. The left panel is the CPL model, right is CTL.

orbiting brown dwarfs and white dwarfs are even more likely to be synchronous rotators, but their potential habitability is further complicated by the luminosity evolution of the central body (Barnes and Heller 2013).

Current technology favors the detection of habitable planets that orbit close to their host star, and hence the planets are more likely to be tidally locked than Earth. This expectation is borne out by the simulations presented in § 3. Proxima b will be a prime target for future observations, and it is almost assuredly tidally locked, and it is highly likely that all potentially habitable *TESS* planets will be tidally locked. The *JWST* telescope may be able to spectroscopically characterize the atmosphere of a few *TESS* planets, and so any biosignature search should consider the role of tidal locking.

Both the CPL and CTL models predict that fast rotation can cause eccentricity growth, but in most cases such growth is modest, acting primarily to delay circularization. This delay can be significant and thus studies that use current orbits to estimate tidal parameters (Jackson et al. 2008; Matsumura et al. 2010) may incorrectly constrain the dissipation rates because they did not take into account the role of rotation. The initial rotation rate is unknown in the vast majority of cases, and so constraining the orbital history of a planet that is currently on a circular orbit and synchronously rotating is very challenging.

For $e \lesssim 0.12$, the exoplanet is likely to be trapped in a 1:1 spin-orbit resonance (Rodríguez et al. 2012), as is the case for Earth’s Moon with $e = 0.05$. However, the position of the host body will not be fixed in the sky, but will librate due to the changing orbital angular velocity and the torques that try to drive the tidally-locked body into a super-synchronous state (Makarov et al. 2016). Given the propensity of M dwarf planets to be multiple (Ballard and Johnson 2016), planets in their HZs will

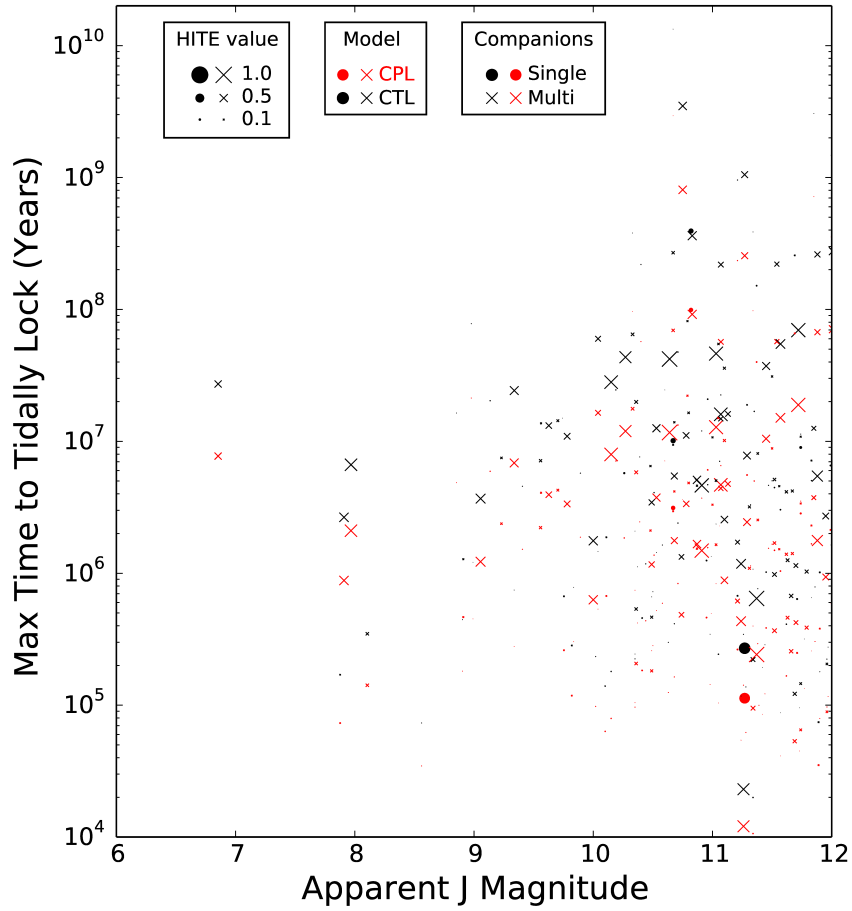


Fig. 10 Maximum timescale for tidal locking, HITE values and apparent J band magnitudes of potentially habitable planets predicted for *TESS* from Sullivan et al. (2015). The tidal locking time assumes a tidal Q of 100, and initial rotation periods and obliquities of 8 hr and 60° , respectively. The circles correspond to planets for which only one planet is detected, x's correspond to planets in multiplanet systems. Dot and x sizes are proportional to the HITE value.

likely have nonzero eccentricities due to mutual gravitational perturbations. Thus, the climates of librating planets should be modeled to determine how libration affects the limits of habitability.

The role of rotation is critical for planetary habitability, and could also be used to discriminate between tidal models. The results presented here show that a more thorough examination of the differences between the CPL and CTL model admits possibilities that could significantly impact our search for life in the universe. As astronomers have focused on discovering habitable exoplanets, a natural synergy will

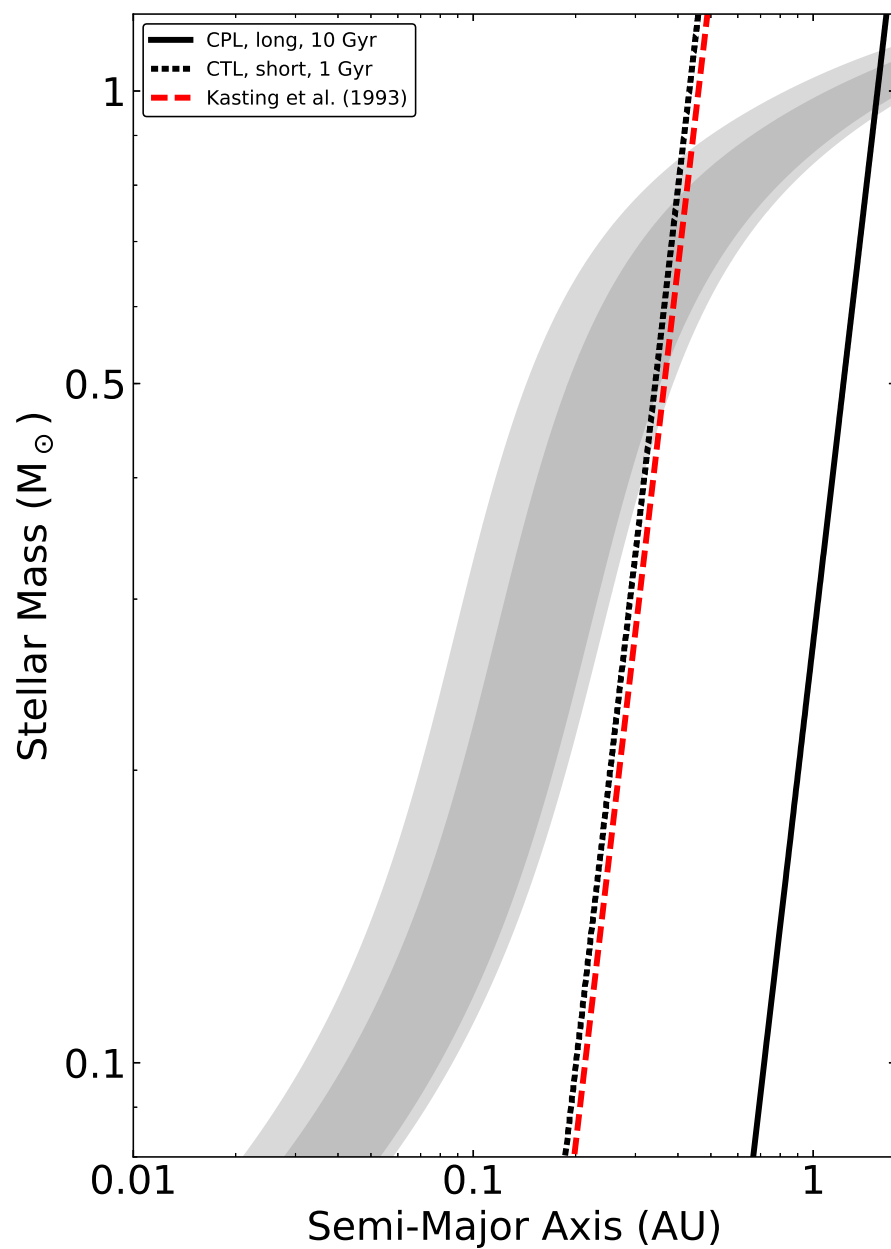


Fig. 11 A comparison of the HZ and the extreme limits for tidal locking obtained in this study and Kasting et al. (1993). The grey regions are the HZ as shown in previous figures. The dashed red curve is the tidal lock radius for the model used by Kasting et al. (1993) (Earth-mass, 13.5 day period, 4.5 Gyr age). The dotted black line is for a 1 Earth-mass planet with an initial spin period of 8 hr and obliquity of 60° and 1 Gyr. The solid black line is for the CPL.

emerge between measuring rotation rates and constraining tidal evolution. When numerous planetary rotation rates of habitable exoplanets have been measured, the nature of tidal evolution may also be revealed.

Acknowledgements This work was supported by NSF grant AST-1108882 and by the NASA Astrobiology Institute's Virtual Planetary Laboratory under Cooperative Agreement number NNA13AA93A. I thank Brian Jackson, René Heller, Jérémy Leconte and two anonymous referee for their comments that greatly improved the content and clarity of this manuscript. This research has made use of the NASA Exoplanet Archive, which is operated by the California Institute of Technology, under contract with the National Aeronautics and Space Administration under the Exoplanet Exploration Program. I also thank GitHub for free hosting of the source codes used in this manuscript, available at <https://github.com/RoryBarnes/TideLock>.

References

- Anglada-Escudé, G. et al. A terrestrial planet candidate in a temperate orbit around Proxima Centauri. *Nature*, 536:437–440, August 2016. doi: 10.1038/nature191106.
- Ballard, S. and Johnson, J.A. The Kepler Dichotomy among the M Dwarfs: Half of Systems Contain Five or More Coplanar Planets. *Astrophys. J.*, 816:66, January 2016. doi: 10.3847/0004-637X/816/2/66.
- Baraffe, I. et al. New evolutionary models for pre-main sequence and main sequence low-mass stars down to the hydrogen-burning limit. *Astron. & Astrophys.*, 577:A42, May 2015. doi: 10.1051/0004-6361/201425481.
- Barnes, R. A method to identify the boundary between rocky and gaseous exoplanets from tidal theory and transit durations. *International Journal of Astrobiology*, 14:321–333, April 2015. doi: 10.1017/S1473550413000499.
- Barnes, R. and Heller, R. Habitable Planets Around White and Brown Dwarfs: The Perils of a Cooling Primary. *Astrobiology*, 13:279–291, March 2013. doi: 10.1089/ast.2012.0867.
- Barnes, R. et al. Tides and the Evolution of Planetary Habitability. *Astrobiology*, 8:557–568, June 2008. doi: 10.1089/ast.2007.0204.
- Barnes, R. et al. Tidal Venuses: Triggering a Climate Catastrophe via Tidal Heating. *Astrobiology*, 13:225–250, March 2013. doi: 10.1089/ast.2012.0851.
- Barnes, R., Meadows, V.S. and Evans, N. Comparative Habitability of Transiting Exoplanets. *Astrophys. J.*, 814:91, December 2015. doi: 10.1088/0004-637X/814/2/91.
- Barnes, R. et al. The Habitability of Proxima Centauri b I: Evolutionary Scenarios. *ArXiv e-prints*, August 2016.
- Batalha, N.M. et al. Planetary Candidates Observed by Kepler. III. Analysis of the First 16 Months of Data. *Astrophys. J. Supp.*, 204:24, February 2013. doi: 10.1088/0067-0049/204/2/24.
- Berta-Thompson, Z.K. et al. A rocky planet transiting a nearby low-mass star. *Nature*, 527: 204–207, November 2015. doi: 10.1038/nature15762.
- Borucki, W.J. et al. Kepler-22b: A 2.4 Earth-radius Planet in the Habitable Zone of a Sun-like Star. *Astrophys. J.*, 745:120, February 2012. doi: 10.1088/0004-637X/745/2/120.
- Cheng, W.H., Lee, M.H. and Peale, S.J. Complete tidal evolution of Pluto-Charon. *Icarus*, 233:242–258, May 2014. doi: 10.1016/j.icarus.2014.01.046.
- Correia, A.C.M. The core mantle friction effect on the secular spin evolution of terrestrial planets. *Earth and Planetary Science Letters*, 252:398–412, December 2006. doi: 10.1016/j.epsl.2006.10.007.
- Correia, A.C.M. and Laskar, J. The four final rotation states of Venus. *Nature*, 411:767–770, June 2001. doi: 10.1038/35081000.
- Correia, A.C.M. and Laskar, J. Long-term evolution of the spin of Venus. II. numerical simulations. *Icarus*, 163:24–45, May 2003. doi: 10.1016/S0019-1035(03)00043-5.
- Correia, A.C.M., Levrard, B. and Laskar, J. On the equilibrium rotation of Earth-like extra-solar planets. *Astron. & Astrophys.*, 488:L63–L66, September 2008. doi: 10.1051/0004-6361:200810388.
- Correia, A.C.M. et al. Tidal damping of the mutual inclination in hierarchical systems. *Astron. & Astrophys.*, 553:A39, May 2013. doi: 10.1051/0004-6361/201220482.

- Counselman, III, C.C. Outcomes of Tidal Evolution. *Astrophys. J.*, 180:307–316, February 1973. doi: 10.1086/151964.
- Ćuk, M. Excitation of Lunar Eccentricity by Planetary Resonances. *Science*, 318:244, 2007. doi: 10.1126/science.1146984.
- Ćuk, M. and Stewart, S.T. Making the Moon from a Fast-Spinning Earth: A Giant Impact Followed by Resonant Despinning. *Science*, 338:1047, November 2012. doi: 10.1126/science.1225542.
- Dalcanton, J. et al. From Cosmic Birth to Living Earths: The Future of UVOIR Space Astronomy. *ArXiv e-prints*, July 2015.
- Darwin, G.H. On the Secular Changes in the Elements of the Orbit of a Satellite Revolving about a Tidally Distorted Planet. *Royal Society of London Philosophical Transactions Series I*, 171:713–891, 1880.
- Dhuime, B. et al. A change in the geodynamics of continental growth 3 billion years ago. *Science*, 335(6074):1334–1336, 2012. ISSN 0036-8075. doi: 10.1126/science.1216066.
- Dickey, J.O. et al. Lunar Laser Ranging: A Continuing Legacy of the Apollo Program. *Science*, 265:482–490, July 1994.
- Dole, S.H. *Habitable planets for man*. 1964.
- Driscoll, P.E. and Barnes, R. Tidal Heating of Earth-like Exoplanets around M Stars: Thermal, Magnetic, and Orbital Evolutions. *Astrobiology*, 15:739–760, September 2015. doi: 10.1089/ast.2015.1325.
- Dumusque, X. et al. The Kepler-10 Planetary System Revisited by HARPS-N: A Hot Rocky World and a Solid Neptune-Mass Planet. *Astrophys. J.*, 789:154, July 2014. doi: 10.1088/0004-637X/789/2/154.
- Efroimsky, M. and Makarov, V.V. Tidal Friction and Tidal Lagging. Applicability Limitations of a Popular Formula for the Tidal Torque. *Astrophys. J.*, 764:26, February 2013. doi: 10.1088/0004-637X/764/1/26.
- Efroimsky, M. and Williams, J.G. Tidal torques: a critical review of some techniques. *Celestial Mechanics and Dynamical Astronomy*, 104:257–289, July 2009.
- Egbert, G.D. and Ray, R.D. Significant dissipation of tidal energy in the deep ocean inferred from satellite altimeter data. *Nature*, 405:775–778, June 2000.
- Espinoza, N. et al. A Neptune-sized Exoplanet Consistent with a Pure Rock Composition. *ArXiv e-prints*, January 2016.
- Ferraz-Mello, S. Tidal synchronization of close-in satellites and exoplanets. A rheophysical approach. *Celestial Mechanics and Dynamical Astronomy*, 116:109–140, June 2013. doi: 10.1007/s10569-013-9482-y.
- Ferraz-Mello, S. Tidal synchronization of close-in satellites and exoplanets: II. Spin dynamics and extension to Mercury and exoplanet host stars. *Celestial Mechanics and Dynamical Astronomy*, 122:359–389, August 2015. doi: 10.1007/s10569-015-9624-5.
- Ferraz-Mello, S., Rodríguez, A. and Hussmann, H. Tidal friction in close-in satellites and exoplanets: The Darwin theory re-visited. *Celestial Mechanics and Dynamical Astronomy*, 101:171–201, May 2008.
- Fleming, S.W. et al. Very Low Mass Stellar and Substellar Companions to Solar-like Stars from MARVELS. II. A Short-period Companion Orbiting an F Star with Evidence of a Stellar Tertiary and Significant Mutual Inclination. *Astron. J.*, 144:72, September 2012. doi: 10.1088/0004-6256/144/3/72.
- Gillon, M. et al. Temperate Earth-sized planets transiting a nearby ultracool dwarf star. *Nature*, 533:221–224, May 2016. doi: 10.1038/nature17448.
- Gold, T. and Soter, S. Atmospheric Tides and the Resonant Rotation of Venus. *Icarus*, 11: 356–366, November 1969. doi: 10.1016/0019-1035(69)90068-2.
- Goldreich, P. Final spin states of planets and satellites. *Astron. J.*, 71:1, February 1966. doi: 10.1086/109844.
- Goldreich, P. and Soter, S. Q in the Solar System. *Icarus*, 5:375–389, 1966.
- Gómez Maqueo Chew, Y. et al. Luminosity Discrepancy in the Equal-mass, Pre-main-sequence Eclipsing Binary Par 1802: Non-coevality or Tidal Heating? *Astrophys. J.*, 745:58, January 2012. doi: 10.1088/0004-637X/745/1/58.
- Gómez Maqueo Chew, Y. et al. The EBLM project. II. A very hot, low-mass M dwarf in an eccentric and long-period, eclipsing binary system from the SuperWASP Survey. *Astron. & Astrophys.*, 572:A50, December 2014. doi: 10.1051/0004-6361/201424265.
- Green, J. et al. Explicitly modelled deep-time tidal dissipation and its implication for lunar history. *Earth and Planetary Science Letters*, 461:46 – 53,

2017. ISSN 0012-821X. doi: <http://dx.doi.org/10.1016/j.epsl.2016.12.038>. URL [//www.sciencedirect.com/science/article/pii/S0012821X16307518](http://www.sciencedirect.com/science/article/pii/S0012821X16307518).
- Greenberg, R. Frequency Dependence of Tidal q . *Astrophys. J.*, 698:L42–L45, June 2009.
- Greenberg, R., Van Laerhoven, C. and Barnes, R. Spin-driven tidal pumping: tidally driven changes in planetary spin coupled with secular interactions between planets. *Celestial Mechanics and Dynamical Astronomy*, 117:331–348, December 2013. doi: 10.1007/s10569-013-9518-3.
- Heller, R. and Barnes, R. Exomoon Habitability Constrained by Illumination and Tidal Heating. *Astrobiology*, 13:18–46, January 2013. doi: 10.1089/ast.2012.0859.
- Heller, R. et al. Tidal effects on brown dwarfs: application to the eclipsing binary 2MASS J05352184-0546085. The anomalous temperature reversal in the context of tidal heating. *Astron. & Astrophys.*, 514:A22, May 2010. doi: 10.1051/0004-6361/200912826.
- Heller, R., Leconte, J. and Barnes, R. Tidal obliquity evolution of potentially habitable planets. *Astro. & Astrophys.*, 528:A27+, April 2011.
- Henning, W.G., O’Connell, R.J. and Sasselov, D.D. Tidally Heated Terrestrial Exoplanets: Viscoelastic Response Models. *Astrophys. J.*, 707:1000–1015, December 2009.
- Heward, E.V. Venus. *MacMillan’s Magazine*, 88:131–140, June 1903.
- Hut, P. Tidal evolution in close binary systems. *Astro. & Astrophys.*, 99:126–140, June 1981.
- Jackson, B., Greenberg, R. and Barnes, R. Tidal Evolution of Close-in Extrasolar Planets. *Astrophys. J.*, 678:1396–1406, May 2008.
- Jackson, B., Barnes, R. and Greenberg, R. Observational Evidence for Tidal Destruction of Exoplanets. *Astrophys. J.*, 698:1357–1366, June 2009.
- Joshi, M.M., Haberle, R.M. and Reynolds, R.T. Simulations of the Atmospheres of Synchronously Rotating Terrestrial Planets Orbiting M Dwarfs: Conditions for Atmospheric Collapse and the Implications for Habitability. *Icarus*, 129:450–465, October 1997. doi: 10.1006/icar.1997.5793.
- Kasting, J.F., Whitmire, D.P. and Reynolds, R.T. Habitable Zones around Main Sequence Stars. *Icarus*, 101:108–128, January 1993. doi: 10.1006/icar.1993.1010.
- Kokubo, E. and Ida, S. Formation of Terrestrial Planets from Protoplanets. II. Statistics of Planetary Spin. *Astrophys. J.*, 671:2082–2090, December 2007. doi: 10.1086/522364.
- Kopparapu, R.K. et al. Habitable Zones around Main-sequence Stars: New Estimates. *Astrophys. J.*, 765:131, March 2013. doi: 10.1088/0004-637X/765/2/131.
- Kopparapu, R.k. et al. The Inner Edge of the Habitable Zone for Synchronously Rotating Planets around Low-mass Stars Using General Circulation Models. *Astrophys. J.*, 819:84, March 2016. doi: 10.3847/0004-637X/819/1/84.
- Lambeck, K. Tidal Dissipation in the Oceans: Astronomical, Geophysical and Oceanographic Consequences. *Royal Society of London Philosophical Transactions Series A*, 287:545–594, December 1977. doi: 10.1098/rsta.1977.0159.
- Leconte, J. et al. Is tidal heating sufficient to explain bloated exoplanets? Consistent calculations accounting for finite initial eccentricity. *Astro. & Astrophys.*, 516:A64+, June 2010.
- Leconte, J. et al. Asynchronous rotation of Earth-mass planets in the habitable zone of lower-mass stars. *Science*, 347:632–635, February 2015. doi: 10.1126/science.1258686.
- Levrard, B., Winisdoerffer, C. and Chabrier, G. Falling Transiting Extrasolar Giant Planets. *Astrophys. J. Lett.*, 692:L9–L13, February 2009. doi: 10.1088/0004-637X/692/1/L9.
- Lowell, P. Venus, further proof of the rotation period of. *Mon. Not. Roy. Astron. Soc.*, 57: 402, March 1897. doi: 10.1093/mnras/57.5.402.
- Ma, B. et al. Very-low-mass Stellar and Substellar Companions to Solar-like Stars from Marvells. III. A Short-period Brown Dwarf Candidate around an Active G0IV Subgiant. *Astron. J.*, 145:20, January 2013. doi: 10.1088/0004-6256/145/1/20.
- MacDonald, G.J.F. Tidal Friction. *Reviews of Geophysics and Space Physics*, 2:467–541, 1964. doi: 10.1029/RG002i003p00467.
- Makarov, V.V. Equilibrium Rotation of Semiliquid Exoplanets and Satellites. *Astrophys. J.*, 810:12, September 2015. doi: 10.1088/0004-637X/810/1/12.
- Makarov, V.V., Frouard, J. and Dorland, B. Forced libration of tidally synchronized planets and moons. *Mon. Not. Roy. Astron. Soc.*, 456:665–671, February 2016. doi: 10.1093/mnras/stv2735.
- Malbet, F. et al. Microarcsecond astrometric observatory Theia: from dark matter to compact objects and nearby earths. In *Society of Photo-Optical Instrumentation Engineers (SPIE) Conference Series*, volume 9904 of *SPIE*, page 99042F, July 2016. doi: 10.1117/12.2234425.

- Mardling, R.A. and Lin, D.N.C. Calculating the Tidal, Spin, and Dynamical Evolution of Extrasolar Planetary Systems. *Astrophys. J.*, 573:829–844, July 2002.
- Matsumura, S., Peale, S.J. and Rasio, F.A. Tidal Evolution of Close-in Planets. *Astrophys. J.*, 725:1995–2016, December 2010.
- Mignard, F. The evolution of the lunar orbit revisited. I. *Moon and Planets*, 20:301–315, May 1979. doi: 10.1007/BF00907581.
- Miguel, Y. and Brunini, A. Planet formation: statistics of spin rates and obliquities of extrasolar planets. *Mon. Not. Roy. Astron. Soc.*, 406:1935–1943, August 2010. doi: 10.1111/j.1365-2966.2010.16804.x.
- Mumford, N.W. Intelligence on Mars of Venus. *Popular Astronomy*, 17:497–504, October 1909.
- Murray, C.D. and Dermott, S.F. *Solar system dynamics*. 1999.
- Peale, S.J. Rotation histories of the natural satellites. In Burns, J.A., editor, *IAU Colloq. 28: Planetary Satellites*, pages 87–111, 1977.
- Peale, S.J., Cassen, P. and Reynolds, R.T. Melting of Io by tidal dissipation. *Science*, 203: 892–894, March 1979.
- Pierrehumbert, R.T. A Palette of Climates for Gliese 581g. *Astrophis. J. Lett.*, 726:L8, January 2011. doi: 10.1088/2041-8205/726/1/L8.
- Press, W.H. et al. *Numerical recipes in C. The art of scientific computing*. 1992.
- Rasio, F.A. et al. Tidal Decay of Close Planetary Orbits. *Astrophys. J.*, 470:1187, October 1996. doi: 10.1086/177941.
- Reiners, A., Schüssler, M. and Passegger, V.M. Generalized Investigation of the Rotation-Activity Relation: Favoring Rotation Period instead of Rossby Number. *Astrophys. J.*, 794:144, October 2014. doi: 10.1088/0004-637X/794/2/144.
- Ricker, G.R. et al. Transiting Exoplanet Survey Satellite (TESS). In *Society of Photo-Optical Instrumentation Engineers (SPIE) Conference Series*, volume 9143 of *Society of Photo-Optical Instrumentation Engineers (SPIE) Conference Series*, page 20, August 2014. doi: 10.1117/12.2063489.
- Rodríguez, A. et al. Spin-orbit coupling for tidally evolving super-Earths. *Mon. Not. Roy. Astron. Soc.*, 427:2239–2250, December 2012. doi: 10.1111/j.1365-2966.2012.22084.x.
- Rogers, L.A. Most 1.6 Earth-Radius Planets are Not Rocky. *Astrophys. J.*, 801:41, March 2015. doi: 10.1088/0004-637X/801/1/41.
- Schiaparelli, G.V. Considerazioni sul Moto Rotatorio del Pianeta Venere. *Memorie della Societa Degli Spettroscopisti Italiani*, 19:220–221, 1891.
- See, T.J.J. The Rotation of Venus and Life on Planets Other Than the Earth. *Popular Astronomy*, 18:1–3, January 1910.
- Selsis, F. et al. Habitable planets around the star Gliese 581? *Astro. & Astrophys.*, 476: 1373–1387, December 2007.
- Shields, A.L. et al. *Astrobiology*, 2016.
- Slipher, V.M. A Spectrographic Investigation of the Rotation Velocity of Venus. *Astronomische Nachrichten*, 163:35, August 1903. doi: 10.1002/asna.19031630303.
- Sotin, C., Grasset, O. and Mocquet, A. Mass radius curve for extrasolar Earth-like planets and ocean planets. *Icarus*, 191:337–351, November 2007.
- Sullivan, P.W. et al. The Transiting Exoplanet Survey Satellite: Simulations of planet detections and astrophysical false positives. *ArXiv e-prints*, June 2015.
- Touma, J. and Wisdom, J. Evolution of the Earth-Moon system. *Astron. J.*, 108:1943–1961, November 1994. doi: 10.1086/117209.
- Van Laerhoven, C., Barnes, R. and Greenberg, R. Tides, planetary companions, and habitability: habitability in the habitable zone of low-mass stars. *Mon. Not. Roy. Astron. Soc.*, 441:1888–1898, July 2014. doi: 10.1093/mnras/stu685.
- Way, M.J. et al. Exploring the Inner Edge of the Habitable Zone with Fully Coupled Oceans. *ArXiv e-prints*, November 2015.
- Webster, A. *The Dynamics of Particles and of Rigid, Elastic, and Fluid Bodies*. Leipzig : B. G. Teubner, 1925.
- Webster, D.L. Meteorological, Geological, and Biological Conditions on Venus. *Nature*, 120: 879–880, December 1927. doi: 10.1038/120879a0.
- Williams, J.G., Sinclair, W.S. and Yoder, C.F. Tidal acceleration of the moon. *Geophys. Rev. Lett.*, 5:943–946, November 1978. doi: 10.1029/GL005i011p00943.
- Wisdom, J. Tidal dissipation at arbitrary eccentricity and obliquity. *Icarus*, 193:637–640, February 2008. doi: 10.1016/j.icarus.2007.09.002.

-
- Wordsworth, R.D. et al. Gliese 581d is the First Discovered Terrestrial-mass Exoplanet in the Habitable Zone. *Astrophys. J. Lett.*, 733:L48, June 2011. doi: 10.1088/2041-8205/733/2/L48.
- Wu, Y. and Goldreich, P. Tidal Evolution of the Planetary System around HD 83443. *Astrophys. J.*, 564:1024–1027, January 2002. doi: 10.1086/324193.
- Yang, J., Cowan, N.B. and Abbot, D.S. Stabilizing Cloud Feedback Dramatically Expands the Habitable Zone of Tidally Locked Planets. *Astrophys. J. Lett.*, 771:L45, July 2013. doi: 10.1088/2041-8205/771/2/L45.
- Yoder, C.F. Astrometric and Geodetic Properties of Earth and the Solar System. In T. J. Ahrens, editor, *Global Earth Physics: A Handbook of Physical Constants*, pages 1–31, 1995.
- Zahnle, K.J. et al. The tethered Moon. *Earth and Planetary Science Letters*, 427, October 2015. doi: 10.1016/j.epsl.2015.06.058.

Table 2: Orbital and Physical Parameters for Projected Isolated Exoplanets from
TESS

ID	R_* (R_\odot)	M_* (M_\odot)	P_{orb} (d)	R_p (R_\oplus)	M_p (M_\oplus)	a (AU)	HTE	T_{CPL}^{short} (Myr)	T_{CPL}^\oplus (Myr)	T_{CPL}^{long} (Myr)	T_{CTL}^{short} (Myr)	T_{CTL}^\oplus (Myr)	T_{CTL}^{long} (Myr)
105	0.14	0.14	7.58	1.68	6.70	0.04	0.66	0.003	0.010	0.113	0.003	0.084	0.270
606	0.56	0.58	42.19	1.82	8.99	0.20	0.26	11.713	11.629	99.198	11.713	136.965	393.163
724	0.39	0.40	15.50	2.42	25.29	0.09	0.02	0.126	0.245	2.284	0.126	2.307	7.062
855	0.35	0.35	17.56	1.87	9.86	0.09	0.27	0.210	0.344	3.130	0.210	3.327	10.114
946	0.29	0.29	12.55	2.09	14.79	0.07	0.15	0.030	0.094	0.913	0.030	0.849	2.634
1344	0.33	0.33	11.52	2.43	25.52	0.07	0.01	0.012	0.073	0.722	0.012	0.647	2.019
1450	0.28	0.27	16.50	2.33	22.02	0.08	0.12	0.178	0.309	2.841	0.178	2.947	8.984
1515	0.26	0.25	7.18	2.04	13.57	0.05	0.03	0.003	0.009	0.104	0.003	0.075	0.243
1753	0.17	0.15	9.36	2.11	15.24	0.05	0.27	0.000	0.028	0.295	0.000	0.242	0.764
1899	0.43	0.45	15.59	1.70	6.86	0.09	0.08	0.105	0.199	1.853	0.105	1.878	5.742

Table 1: Orbital and Physical Parameters for Potentially Habitable, Isolated *Kepler* Candidates

Name	R_* (R_\odot)	M_* (M_\odot)	P_{orb} (d)	R_p (R_\oplus)	M_p (M_\oplus)	a (AU)	HTE	T_{CPL}^{short} (Gyr)	T_{CPL}^\oplus (Gyr)	T_{CPL}^{long} (Gyr)	T_{CTL}^{short} (Gyr)	T_{CTL}^\oplus (Gyr)	T_{CTL}^{long} (Gyr)
Kepler-22b	0.98	0.96	289.86	2.39	24.23	0.85	0.09	1.011	15.000	15.000	15.000	15.000	15.000
K00174.01	0.67	0.65	56.35	2.37	23.38	0.25	0.02	0.001	0.044	0.375	0.053	0.552	1.563
K00227.01	0.47	0.49	17.66	2.38	23.70	0.10	0.01	0.000	0.000	0.004	0.000	0.004	0.012
K00463.01	0.30	0.30	18.48	1.73	7.40	0.09	0.53	0.000	0.000	0.004	0.000	0.004	0.012
K00494.01	0.48	0.50	25.70	1.79	8.31	0.14	0.18	0.000	0.002	0.013	0.001	0.016	0.049
Kepler-225c	0.48	0.51	18.79	2.15	16.40	0.11	0.05	0.000	0.000	0.004	0.000	0.005	0.015
Kepler-231c	0.49	0.53	19.27	1.95	11.35	0.11	0.05	0.000	0.001	0.005	0.000	0.005	0.015
Kepler-236c	0.51	0.53	23.97	2.01	12.85	0.13	0.10	0.000	0.001	0.011	0.001	0.013	0.039
K00854.01	0.47	0.49	56.06	2.18	17.22	0.23	0.28	0.001	0.041	0.348	0.048	0.512	1.448
Kepler-55c	0.62	0.67	42.15	2.35	22.61	0.21	0.02	0.000	0.014	0.117	0.015	0.160	0.462
K00947.01	0.46	0.49	28.60	2.05	13.85	0.14	0.19	0.000	0.003	0.023	0.002	0.028	0.083
K00959.01	0.12	0.09	12.71	2.44	26.08	0.05	0.02	0.000	0.000	0.001	0.000	0.001	0.003
K01058.01	0.18	0.16	5.67	0.53	0.13	0.03	0.04	0.000	0.000	0.000	0.000	0.000	0.000
K01725.01	0.32	0.32	9.89	1.37	3.16	0.06	0.04	0.000	0.000	0.000	0.000	0.000	0.001
K01871.01	0.62	0.65	92.73	2.44	25.81	0.35	0.05	0.010	0.326	2.802	0.452	4.602	12.659
K01938.01	0.70	0.78	96.92	2.21	17.96	0.38	0.08	0.011	0.364	3.134	0.518	5.200	14.256
K01989.01	0.84	0.82	201.12	2.01	12.68	0.63	0.20	0.205	6.247	15.000	10.380	15.000	15.000
K02020.01	0.55	0.54	110.97	2.17	16.77	0.37	0.32	0.019	0.616	5.324	0.895	9.067	15.000
K02124.01	0.55	0.56	42.34	1.15	1.69	0.20	0.34	0.000	0.009	0.075	0.010	0.103	0.297
Kepler-369c	0.47	0.50	14.87	1.61	5.71	0.09	0.04	0.000	0.000	0.001	0.000	0.001	0.005
K02290.01	0.72	0.79	91.50	2.05	13.86	0.37	0.12	0.008	0.276	2.377	0.386	3.891	10.710
K02373.01	0.83	0.87	147.28	2.03	13.19	0.52	0.14	0.058	1.821	15.000	2.828	15.000	15.000
K02401.01	0.60	0.59	38.23	1.56	5.10	0.19	0.03	0.000	0.007	0.060	0.008	0.081	0.235
K02418.01	0.41	0.43	86.83	1.32	2.73	0.29	0.56	0.005	0.168	1.443	0.227	2.341	6.457
K02469.01	0.64	0.69	131.19	2.26	19.59	0.45	0.24	0.039	1.233	10.696	1.893	15.000	15.000
K02474.01	0.80	0.81	176.85	1.81	8.65	0.57	0.31	0.114	3.498	15.000	5.737	15.000	15.000
K02554.01	0.51	0.52	39.76	1.42	3.59	0.18	0.18	0.000	0.008	0.066	0.008	0.090	0.260
K02626.01	0.35	0.36	38.10	1.22	2.05	0.16	0.89	0.000	0.006	0.051	0.006	0.068	0.197
Kepler-395c	0.56	0.61	34.99	1.56	5.12	0.18	0.12	0.000	0.005	0.042	0.005	0.056	0.163
K02760.01	0.64	0.67	56.57	1.95	11.46	0.25	0.14	0.001	0.039	0.335	0.047	0.495	1.399
K02862.01	0.49	0.51	24.58	1.69	6.86	0.13	0.17	0.000	0.001	0.011	0.001	0.013	0.039
K02882.01	0.61	0.64	75.86	2.41	24.92	0.30	0.05	0.004	0.145	1.246	0.192	1.964	5.454
K02931.01	0.75	0.76	99.25	1.90	10.46	0.38	0.14	0.011	0.363	3.131	0.516	5.213	14.282
K02992.01	0.55	0.57	82.66	2.48	27.47	0.31	0.02	0.006	0.208	1.788	0.284	2.870	7.939
K03010.01	0.52	0.54	60.87	1.73	7.34	0.25	0.75	0.001	0.049	0.415	0.060	0.622	1.754
K03034.01	0.52	0.54	31.02	1.73	7.37	0.16	0.20	0.000	0.003	0.028	0.003	0.036	0.105
K03138.01	0.12	0.10	8.69	0.62	0.21	0.04	0.74	0.000	0.000	0.000	0.000	0.000	0.000
Kepler-437b	0.68	0.72	66.65	1.68	6.59	0.29	0.24	0.002	0.068	0.586	0.087	0.897	2.509
K03266.01	0.61	0.61	54.51	1.74	7.53	0.24	0.21	0.001	0.031	0.268	0.038	0.392	1.111
K03282.01	0.54	0.55	49.28	2.19	17.40	0.22	0.22	0.001	0.024	0.208	0.028	0.297	0.847
Kepler-438b	0.52	0.54	35.23	1.14	1.60	0.17	0.42	0.000	0.004	0.035	0.004	0.047	0.136
K03391.01	0.54	0.53	36.77	1.56	5.04	0.18	0.11	0.000	0.006	0.052	0.006	0.069	0.200
K03407.01	0.74	0.81	92.44	2.34	22.31	0.37	0.01	0.009	0.313	2.696	0.438	4.430	12.175
K03443.01	0.71	0.76	96.17	2.35	22.76	0.38	0.03	0.011	0.368	3.170	0.520	5.244	14.391
K03508.01	0.99	1.04	190.80	1.82	8.82	0.66	0.06	0.155	4.748	15.000	7.892	15.000	15.000
K03966.01	0.84	0.93	138.94	2.13	15.75	0.51	0.04	0.047	1.491	12.946	2.312	15.000	15.000
K04036.01	0.76	0.74	168.81	2.05	13.81	0.54	0.43	0.102	3.160	15.000	5.104	15.000	15.000
K04054.01	0.78	0.86	169.13	2.20	17.84	0.57	0.19	0.108	3.332	15.000	5.394	15.000	15.000
K04060.01	0.89	0.93	225.26	2.09	14.71	0.71	0.17	0.334	10.072	15.000	15.000	15.000	15.000
Kepler-440b	0.56	0.59	101.11	1.90	10.45	0.36	0.53	0.012	0.391	3.372	0.559	5.638	15.000
K04103.01	0.68	0.71	184.77	2.38	23.51	0.57	0.12	0.162	4.976	15.000	8.161	15.000	15.000
K04242.01	0.99	1.10	145.79	2.22	18.48	0.56	0.02	0.059	1.857	15.000	2.896	15.000	15.000
K04290.01	0.16	0.13	4.84	0.83	0.54	0.03	0.15	0.000	0.000	0.000	0.000	0.000	0.000
K04307.01	0.97	0.95	160.85	2.30	21.06	0.57	0.01	0.091	2.811	15.000	4.448	15.000	15.000

Table 1 (con't)

Name	R_* (R_\odot)	M_* (M_\odot)	P_{orb} (d)	R_p (R_\oplus)	M_p (M_\oplus)	a (AU)	HTE	T_{CPL}^{short} (Gyr)	T_{CPL}^\oplus (Gyr)	T_{CPL}^{long} (Gyr)	T_{CTL}^{short} (Gyr)	T_{CTL}^\oplus (Gyr)	T_{CTL}^{long} (Gyr)
K04333.01	1.06	1.07	309.26	2.37	23.21	0.92	0.07	1.303	15.000	15.000	15.000	15.000	15.000
K04356.01	0.46	0.50	174.51	2.07	14.24	0.48	0.18	0.118	3.626	15.000	5.880	15.000	15.000
K04367.01	0.95	1.02	170.99	2.38	23.86	0.61	0.01	0.119	3.665	15.000	5.865	15.000	15.000
K04426.01	1.45	1.08	369.13	2.32	21.66	1.03	0.03	2.629	15.000	15.000	15.000	15.000	15.000
K04450.01	0.82	0.89	196.44	2.19	17.61	0.64	0.20	0.198	6.030	15.000	9.957	15.000	15.000
K04460.01	0.96	0.87	284.73	2.28	20.29	0.81	0.14	0.912	15.000	15.000	15.000	15.000	15.000
K04550.01	0.70	0.68	140.25	1.91	10.68	0.46	0.54	0.046	1.444	12.543	2.239	15.000	15.000
K04583.01	0.77	0.84	330.91	2.28	20.31	0.88	0.19	1.673	15.000	15.000	15.000	15.000	15.000
Kepler-441b	0.55	0.57	207.25	1.79	8.33	0.57	0.31	0.215	6.532	15.000	11.000	15.000	15.000
Kepler-442b	0.60	0.61	112.31	1.62	5.84	0.39	0.84	0.017	0.536	4.628	0.777	7.898	15.000
Kepler-443b	0.71	0.75	177.67	2.35	22.75	0.56	0.13	0.138	4.233	15.000	6.850	15.000	15.000
K04810.01	0.87	0.97	115.24	2.26	19.64	0.46	0.02	0.023	0.737	6.369	1.086	10.925	15.000
K04878.01	1.07	0.97	449.01	1.13	1.57	1.14	0.80	3.625	15.000	15.000	15.000	15.000	15.000
K04902.01	0.80	0.77	409.39	2.01	12.77	0.99	0.28	3.631	15.000	15.000	15.000	15.000	15.000
K04926.01	0.70	0.68	69.08	1.67	6.49	0.29	0.12	0.002	0.079	0.674	0.100	1.040	2.907
K04961.01	0.79	0.84	348.96	2.09	14.74	0.91	0.24	1.958	15.000	15.000	15.000	15.000	15.000
K04986.01	0.73	0.81	444.04	1.62	5.79	1.06	0.65	4.375	15.000	15.000	15.000	15.000	15.000
K04991.01	0.91	1.00	211.33	2.29	20.57	0.69	0.08	0.274	8.293	15.000	13.946	15.000	15.000
K05068.01	1.05	0.92	385.29	1.70	6.90	1.01	0.36	2.549	15.000	15.000	15.000	15.000	15.000
K05087.01	1.26	0.96	651.07	1.71	7.01	1.45	0.73	15.000	15.000	15.000	15.000	15.000	15.000
K05098.01	0.90	0.82	100.35	1.73	7.39	0.39	0.04	0.011	0.357	3.075	0.506	5.130	14.050
K05101.01	1.50	0.99	436.19	1.77	8.10	1.12	0.11	4.322	15.000	15.000	15.000	15.000	15.000
K05121.01	1.91	1.39	401.20	2.27	19.91	1.19	0.03	3.623	15.000	15.000	15.000	15.000	15.000
K05135.01	0.76	0.83	314.77	2.23	18.62	0.85	0.22	1.346	15.000	15.000	15.000	15.000	15.000
K05164.01	1.04	1.09	209.97	1.25	2.23	0.71	0.08	0.179	5.438	15.000	9.177	15.000	15.000
K05176.01	0.86	0.81	215.73	1.35	2.97	0.65	0.40	0.211	6.377	15.000	10.928	15.000	15.000
K05196.01	1.13	1.15	392.47	2.39	24.18	1.10	0.05	3.433	15.000	15.000	15.000	15.000	15.000
K05202.01	0.96	1.04	535.94	1.92	10.79	1.31	0.51	10.418	15.000	15.000	15.000	15.000	15.000
K05236.01	1.03	1.09	550.86	2.15	16.25	1.35	0.34	12.513	15.000	15.000	15.000	15.000	15.000
K05237.01	0.74	0.82	380.39	2.00	12.45	0.96	0.43	2.689	15.000	15.000	15.000	15.000	15.000
K05248.01	0.82	0.77	179.25	1.48	4.14	0.57	0.33	0.105	3.238	15.000	5.295	15.000	15.000
K05254.01	1.50	1.05	232.92	1.31	2.71	0.75	0.02	0.283	8.511	15.000	14.794	15.000	15.000
K05276.01	0.70	0.75	220.72	2.45	26.46	0.65	0.04	0.341	10.313	15.000	15.000	15.000	15.000
K05279.01	0.84	0.89	103.72	1.69	6.75	0.42	0.03	0.012	0.401	3.455	0.569	5.812	15.000
K05290.01	0.88	0.98	435.51	2.26	19.74	1.12	0.20	5.034	15.000	15.000	15.000	15.000	15.000
K05372.01	1.21	1.02	212.60	1.81	8.68	0.70	0.09	0.240	7.283	15.000	12.230	15.000	15.000
K05387.01	0.59	0.58	297.78	1.27	2.43	0.73	0.02	0.749	15.000	15.000	15.000	15.000	15.000
K05398.01	0.89	1.00	551.22	2.31	21.29	1.32	0.13	13.165	15.000	15.000	15.000	15.000	15.000
K05413.01	0.95	0.80	428.38	2.04	13.59	1.03	0.42	4.407	15.000	15.000	15.000	15.000	15.000
K05475.01	0.81	0.85	448.30	1.79	8.41	1.08	0.64	4.859	15.000	15.000	15.000	15.000	15.000
K05476.01	0.93	1.02	148.17	2.35	22.50	0.55	0.02	0.066	2.052	15.000	3.179	15.000	15.000
K05499.01	0.67	0.65	122.58	1.30	2.63	0.42	0.53	0.021	0.658	5.700	0.980	9.908	15.000
K05506.01	1.03	1.09	641.60	1.73	7.43	1.50	0.69	15.000	15.000	15.000	15.000	15.000	15.000
K05528.01	0.92	0.94	201.62	2.21	17.95	0.66	0.09	0.221	6.712	15.000	11.217	15.000	15.000
K05541.01	0.90	0.98	339.63	2.24	18.87	0.95	0.26	1.834	15.000	15.000	15.000	15.000	15.000
K05545.01	0.80	0.88	541.04	1.18	1.82	1.25	0.69	7.883	15.000	15.000	15.000	15.000	15.000
K05554.01	1.28	0.88	362.22	1.01	1.03	0.95	0.22	1.417	15.000	15.000	15.000	15.000	15.000
K05556.01	1.01	0.90	631.99	2.04	13.49	1.39	0.34	15.000	15.000	15.000	15.000	15.000	15.000
K05568.01	0.92	1.01	186.40	1.14	1.62	0.64	0.10	0.104	3.199	15.000	5.295	15.000	15.000
K05570.01	0.82	0.88	574.65	2.41	24.84	1.30	0.05	15.000	15.000	15.000	15.000	15.000	15.000
K05623.01	1.12	1.08	583.76	2.17	16.84	1.40	0.32	15.000	15.000	15.000	15.000	15.000	15.000
K05638.01	1.15	1.16	290.02	1.64	6.15	0.90	0.18	0.794	15.000	15.000	15.000	15.000	15.000
K05651.01	0.77	0.73	83.50	1.81	8.69	0.34	0.07	0.005	0.177	1.517	0.242	2.437	6.735
K05652.01	0.63	0.62	91.51	1.59	5.37	0.34	0.30	0.007	0.234	2.009	0.326	3.292	9.049

Table 1 (con't)

Name	R_* (R_\odot)	M_* (M_\odot)	P_{orb} (d)	R_p (R_\oplus)	M_p (M_\oplus)	a (AU)	HITE	T_{CPL}^{short} (Gyr)	T_{CPL}^\oplus (Gyr)	T_{CPL}^{long} (Gyr)	T_{CTL}^{short} (Gyr)	T_{CTL}^\oplus (Gyr)	T_{CTL}^{long} (Gyr)
K05653.01	0.67	0.65	188.66	2.27	19.96	0.56	0.21	0.172	5.252	15.000	8.591	15.000	15.000
K05657.01	1.03	1.03	284.70	2.16	16.63	0.85	0.15	0.879	15.000	15.000	15.000	15.000	15.000
K05666.01	0.93	0.95	182.45	1.37	3.17	0.62	0.13	0.108	3.312	15.000	5.484	15.000	15.000
K05671.01	1.13	0.98	190.91	1.86	9.62	0.64	0.03	0.158	4.833	15.000	7.990	15.000	15.000
K05694.01	0.80	0.88	107.90	1.38	3.25	0.42	0.11	0.013	0.412	3.553	0.591	6.015	15.000
K05704.01	0.72	0.77	96.17	1.28	2.50	0.38	0.23	0.008	0.248	2.138	0.351	3.539	9.716
K05736.01	0.84	0.92	161.65	1.45	3.87	0.57	0.24	0.068	2.120	15.000	3.398	15.000	15.000
K05737.01	0.96	0.98	376.24	1.43	3.66	1.01	0.92	2.069	15.000	15.000	15.000	15.000	15.000
K05749.01	0.69	0.74	281.95	2.43	25.67	0.76	0.04	0.914	15.000	15.000	15.000	15.000	15.000
K05758.01	0.79	0.87	102.49	2.18	17.08	0.41	0.08	0.014	0.451	3.886	0.641	6.510	15.000
K05798.01	0.76	0.83	318.26	2.28	20.13	0.86	0.17	1.427	15.000	15.000	15.000	15.000	15.000
K05801.01	0.92	1.01	177.38	2.15	16.32	0.62	0.10	0.129	3.963	15.000	6.463	15.000	15.000
K05806.01	0.97	0.98	313.83	1.38	3.20	0.90	0.63	0.972	15.000	15.000	15.000	15.000	15.000
K05810.01	1.44	0.93	425.59	2.42	25.28	1.08	0.05	4.796	15.000	15.000	15.000	15.000	15.000
K05819.01	0.73	0.80	381.38	1.35	2.96	0.95	0.76	2.103	15.000	15.000	15.000	15.000	15.000
K05825.01	1.20	0.79	208.05	2.22	18.35	0.63	0.01	0.252	7.635	15.000	12.897	15.000	15.000
K05829.01	0.86	0.98	583.85	2.08	14.45	1.36	0.24	15.000	15.000	15.000	15.000	15.000	15.000
K05856.01	0.85	0.77	259.34	1.77	8.10	0.73	0.40	0.531	15.000	15.000	15.000	15.000	15.000
K05885.01	0.95	1.06	111.15	2.05	13.81	0.46	0.01	0.019	0.599	5.176	0.867	8.825	15.000
K05888.01	0.80	0.89	190.86	1.98	12.14	0.62	0.35	0.165	5.033	15.000	8.313	15.000	15.000
K05902.01	0.87	0.97	150.73	1.39	3.31	0.55	0.19	0.050	1.561	13.582	2.467	15.000	15.000
K05918.01	0.87	0.87	94.68	1.60	5.56	0.39	0.05	0.008	0.269	2.316	0.375	3.823	10.504
K05938.01	1.16	1.08	545.21	1.78	8.21	1.34	0.66	10.630	15.000	15.000	15.000	15.000	15.000
K05948.01	0.76	0.83	398.51	1.31	2.66	1.00	0.84	2.464	15.000	15.000	15.000	15.000	15.000
K05949.01	1.11	1.01	559.79	2.01	12.76	1.33	0.48	12.786	15.000	15.000	15.000	15.000	15.000
K05950.01	0.74	0.82	109.44	1.11	1.44	0.42	0.21	0.012	0.377	3.253	0.550	5.533	15.000
K05952.01	1.02	0.91	164.51	2.32	21.49	0.57	0.02	0.100	3.085	15.000	4.971	15.000	15.000
K05959.01	0.90	0.98	251.49	1.72	7.21	0.78	0.40	0.459	13.755	15.000	15.000	15.000	15.000
K06108.01	0.96	0.81	485.92	1.16	1.70	1.13	0.87	5.057	15.000	15.000	15.000	15.000	15.000
K06151.01	0.75	0.81	431.79	1.49	4.24	1.04	0.74	3.698	15.000	15.000	15.000	15.000	15.000
K06239.01	0.88	0.95	406.50	1.88	10.02	1.06	0.58	3.379	15.000	15.000	15.000	15.000	15.000
K06343.01	0.95	1.02	569.45	2.19	17.37	1.36	0.27	14.470	15.000	15.000	15.000	15.000	15.000
K06425.01	0.95	0.88	521.11	1.57	5.22	1.22	0.84	8.179	15.000	15.000	15.000	15.000	15.000
K06610.01	0.84	0.77	315.08	2.43	25.64	0.83	0.07	1.431	15.000	15.000	15.000	15.000	15.000
K06676.01	0.96	1.02	439.25	1.93	11.06	1.14	0.44	4.699	15.000	15.000	15.000	15.000	15.000
K06971.01	0.79	0.76	129.22	1.87	9.89	0.46	0.29	0.032	1.028	8.912	1.543	15.000	15.000
Kepler-452b	1.11	0.94	384.84	1.71	7.06	1.01	0.60	2.547	15.000	15.000	15.000	15.000	15.000
K07040.01	0.73	0.81	502.23	1.56	5.13	1.15	0.70	7.026	15.000	15.000	15.000	15.000	15.000
K07073.01	1.14	1.08	278.99	1.96	11.70	0.86	0.11	0.761	15.000	15.000	15.000	15.000	15.000
K07099.01	0.50	0.50	34.04	1.08	1.34	0.16	0.09	0.000	0.003	0.030	0.004	0.039	0.114
K07179.01	1.20	1.00	407.12	1.28	2.48	1.08	0.61	2.652	15.000	15.000	15.000	15.000	15.000
K07223.01	0.73	0.77	317.05	1.81	8.77	0.83	0.57	1.212	15.000	15.000	15.000	15.000	15.000
K07235.01	0.76	0.83	299.67	1.24	2.17	0.82	0.93	0.752	15.000	15.000	15.000	15.000	15.000
K07345.01	1.02	1.09	377.50	2.41	24.98	1.05	0.07	2.952	15.000	15.000	15.000	15.000	15.000
K07470.01	0.99	0.87	392.51	2.18	17.13	1.00	0.28	3.230	15.000	15.000	15.000	15.000	15.000
K07554.01	1.09	1.07	482.61	2.20	17.84	1.23	0.26	7.474	15.000	15.000	15.000	15.000	15.000
K07587.01	0.94	0.95	366.09	2.29	20.66	0.98	0.20	2.521	15.000	15.000	15.000	15.000	15.000
K07591.01	0.67	0.72	328.33	1.39	3.36	0.84	0.52	1.176	15.000	15.000	15.000	15.000	15.000
K07617.01	0.38	0.40	12.93	0.69	0.30	0.08	0.05	0.000	0.000	0.001	0.000	0.001	0.002

Table 3: Orbital and Physical Parameters for Projected Exoplanets in Multi-Planet Systems from *TESS*

ID	R_* (R_\odot)	M_* (M_\odot)	P_{orb} (d)	R_p (R_\oplus)	M_p (M_\oplus)	a (AU)	HTE	T_{CPL}^{short} (Myr)	T_{CPL}^\oplus (Myr)	T_{CPL}^{long} (Myr)	T_{CTL}^{short} (Myr)	T_{CTL}^\oplus (Myr)	T_{CTL}^{long} (Myr)
2	0.32	0.33	14.20	2.19	17.40	0.08	0.11	0.001	0.160	1.521	0.070	1.484	4.575
6	0.32	0.32	13.99	2.32	21.72	0.08	0.06	0.001	0.157	1.493	0.069	1.446	4.463
11	0.22	0.21	11.45	1.97	11.97	0.06	0.28	0.000	0.062	0.616	0.008	0.553	1.722
25	0.26	0.26	15.14	1.71	7.10	0.08	0.50	0.001	0.178	1.664	0.090	1.667	5.106
27	0.22	0.20	17.18	2.40	24.38	0.08	0.10	0.004	0.370	3.382	0.223	3.564	10.844
35	0.33	0.35	10.35	2.12	15.58	0.07	0.04	0.000	0.043	0.436	0.000	0.374	1.177
43	0.42	0.45	19.54	1.98	12.08	0.11	0.14	0.007	0.551	4.837	0.372	5.442	16.452
45	0.16	0.14	15.96	1.05	1.19	0.06	0.87	0.001	0.160	1.485	0.086	1.517	4.636
48	0.16	0.13	12.55	1.99	12.39	0.05	0.45	0.000	0.091	0.885	0.029	0.822	2.552
49	0.31	0.33	7.68	2.27	19.80	0.05	0.01	0.000	0.013	0.144	0.004	0.108	0.345
67	0.19	0.17	5.63	2.08	14.36	0.03	0.06	0.000	0.003	0.041	0.002	0.027	0.087
78	0.25	0.24	9.66	1.41	3.50	0.06	0.25	0.000	0.025	0.256	0.000	0.213	0.674
81	0.18	0.16	5.87	2.14	16.12	0.03	0.07	0.000	0.004	0.049	0.002	0.032	0.106
89	0.33	0.35	15.68	2.29	20.41	0.09	0.09	0.002	0.247	2.300	0.135	2.332	7.152
92	0.28	0.28	14.14	2.28	20.25	0.07	0.11	0.001	0.162	1.536	0.072	1.500	4.610
98	0.23	0.21	5.61	1.64	6.10	0.04	0.02	0.000	0.003	0.035	0.002	0.022	0.073
114	0.26	0.25	7.06	2.03	13.23	0.05	0.03	0.000	0.009	0.097	0.003	0.070	0.225
116	0.18	0.16	6.90	2.05	13.76	0.04	0.14	0.000	0.008	0.089	0.003	0.064	0.205
127	0.26	0.26	9.09	2.08	14.56	0.05	0.08	0.000	0.025	0.261	0.000	0.211	0.669
131	0.39	0.42	17.31	2.45	26.17	0.10	0.02	0.004	0.387	3.521	0.237	3.731	11.342
135	0.12	0.10	18.46	2.42	25.32	0.06	0.01	0.006	0.499	4.419	0.318	4.869	14.768
139	0.21	0.14	8.11	1.60	5.58	0.04	0.20	0.000	0.013	0.142	0.003	0.109	0.348
142	0.25	0.23	16.62	2.38	23.54	0.08	0.11	0.003	0.322	2.957	0.180	3.067	9.357
148	0.41	0.43	35.73	2.15	16.40	0.16	0.34	0.131	6.645	56.761	6.240	75.133	218.715
150	0.25	0.25	8.96	1.30	2.61	0.05	0.17	0.000	0.017	0.182	0.000	0.147	0.465
155	0.32	0.33	10.90	1.72	7.25	0.07	0.10	0.000	0.047	0.465	0.000	0.408	1.279
172	0.17	0.15	15.58	2.28	20.32	0.06	0.20	0.002	0.241	2.244	0.128	2.273	6.950
173	0.29	0.30	7.63	1.90	10.37	0.05	0.02	0.000	0.011	0.125	0.003	0.093	0.299
204	0.24	0.23	14.32	0.77	0.43	0.07	0.57	0.001	0.093	0.882	0.042	0.864	2.656
210	0.29	0.30	25.86	1.59	5.43	0.11	0.85	0.025	1.485	12.799	1.187	15.638	46.302
225	0.44	0.46	20.94	2.34	22.27	0.11	0.05	0.011	0.813	7.096	0.579	8.177	24.544
226	0.17	0.15	13.04	1.96	11.66	0.06	0.52	0.000	0.106	1.017	0.039	0.959	2.970
244	0.37	0.39	23.24	1.17	1.80	0.12	0.54	0.012	0.792	6.861	0.615	8.149	24.263
249	0.30	0.31	49.94	2.43	25.44	0.18	0.04	0.608	27.504	234.545	29.346	336.392	957.291
251	0.25	0.24	15.61	2.10	15.03	0.08	0.32	0.002	0.230	2.141	0.121	2.170	6.636
253	0.45	0.48	37.26	2.26	19.71	0.17	0.19	0.163	8.124	69.375	7.700	92.946	269.200
257	0.33	0.35	39.61	2.42	24.98	0.16	0.07	0.222	10.833	92.447	10.457	125.559	362.576
272	0.16	0.14	5.50	2.05	13.64	0.03	0.16	0.000	0.003	0.037	0.002	0.024	0.078
273	0.40	0.41	17.48	2.11	15.16	0.10	0.10	0.004	0.365	3.312	0.226	3.529	10.723
287	0.23	0.21	21.98	1.72	7.27	0.09	0.69	0.012	0.811	7.050	0.599	8.236	24.660
298	0.23	0.22	12.98	2.25	19.14	0.07	0.17	0.001	0.113	1.091	0.039	1.029	3.185
306	0.40	0.42	16.95	2.11	15.26	0.10	0.09	0.003	0.322	2.952	0.185	3.100	9.410
309	0.21	0.22	5.63	1.64	6.07	0.04	0.09	0.000	0.003	0.035	0.001	0.023	0.074
324	0.36	0.37	10.04	2.40	24.24	0.07	0.01	0.000	0.041	0.420	0.000	0.356	1.120
333	0.39	0.40	12.42	1.94	11.30	0.08	0.05	0.000	0.086	0.836	0.023	0.774	2.403
346	0.29	0.30	7.88	1.90	10.45	0.05	0.03	0.000	0.013	0.142	0.003	0.108	0.344
370	0.39	0.40	24.38	2.42	25.21	0.12	0.05	0.024	1.538	13.295	1.188	15.998	47.511
374	0.20	0.18	16.57	2.09	14.84	0.07	0.39	0.003	0.293	2.694	0.166	2.793	8.516
384	0.40	0.41	11.05	1.89	10.11	0.07	0.01	0.000	0.052	0.521	0.002	0.460	1.436
385	0.30	0.30	7.39	2.05	13.84	0.05	0.01	0.000	0.010	0.116	0.003	0.086	0.275
386	0.52	0.53	70.44	1.95	11.51	0.27	0.51	2.258	94.313	807.069	109.949	1248.874	3488.501
392	0.25	0.24	7.15	2.00	12.51	0.05	0.05	0.000	0.009	0.101	0.003	0.073	0.235
398	0.17	0.15	6.90	2.03	13.28	0.04	0.17	0.000	0.008	0.089	0.003	0.063	0.204
405	0.38	0.40	22.82	1.58	5.27	0.12	0.44	0.013	0.891	7.730	0.680	9.130	27.215

Table 3 (con't)

ID	R_* (R_\odot)	M_* (M_\odot)	P_{orb} (d)	R_p (R_\oplus)	M_p (M_\oplus)	a (AU)	HTE	T_{CPL}^{short} (Myr)	T_{CPL}^\oplus (Myr)	T_{CPL}^{long} (Myr)	T_{CTL}^{short} (Myr)	T_{CTL}^\oplus (Myr)	T_{CTL}^{long} (Myr)
410	0.51	0.54	36.50	1.90	10.43	0.17	0.30	0.133	6.677	57.039	6.293	76.070	220.537
426	0.40	0.42	23.22	2.15	16.43	0.12	0.17	0.018	1.171	10.142	0.876	12.003	35.865
433	0.29	0.30	7.13	2.16	16.65	0.05	0.01	0.000	0.009	0.105	0.003	0.076	0.244
434	0.33	0.35	23.80	1.94	11.25	0.11	0.48	0.019	1.209	10.464	0.937	12.485	37.232
451	0.20	0.19	14.64	2.44	25.82	0.07	0.06	0.001	0.195	1.837	0.090	1.814	5.582
477	0.19	0.16	5.83	2.18	17.25	0.03	0.06	0.000	0.004	0.048	0.002	0.032	0.104
486	0.18	0.16	6.88	1.59	5.47	0.04	0.24	0.000	0.007	0.075	0.003	0.053	0.172
512	0.16	0.05	20.63	2.46	26.84	0.05	0.02	0.011	0.792	6.917	0.547	7.921	23.811
513	0.31	0.33	16.96	1.57	5.20	0.09	0.46	0.003	0.267	2.442	0.161	2.565	7.805
519	0.36	0.38	65.73	2.49	27.89	0.23	0.01	1.978	83.797	716.227	95.629	1091.385	3064.412
530	0.26	0.25	14.58	2.21	18.01	0.07	0.19	0.001	0.180	1.694	0.084	1.674	5.138
543	0.43	0.45	17.06	1.60	5.60	0.10	0.14	0.003	0.277	2.536	0.163	2.659	8.095
547	0.27	0.27	8.23	1.86	9.63	0.05	0.07	0.000	0.015	0.165	0.003	0.128	0.410
578	0.36	0.38	11.23	1.98	12.12	0.07	0.05	0.000	0.058	0.573	0.005	0.510	1.590
581	0.36	0.38	18.55	1.83	9.02	0.10	0.28	0.005	0.424	3.742	0.278	4.144	12.556
582	0.23	0.22	6.88	2.40	24.46	0.04	0.01	0.000	0.009	0.098	0.003	0.069	0.224
583	0.30	0.30	15.34	2.28	20.19	0.08	0.11	0.002	0.226	2.107	0.114	2.121	6.494
588	0.40	0.41	14.46	2.25	19.30	0.09	0.04	0.001	0.176	1.662	0.080	1.635	5.020
600	0.40	0.41	22.27	2.25	19.42	0.12	0.12	0.015	1.019	8.846	0.749	10.362	31.016
611	0.27	0.27	28.36	1.79	8.41	0.12	0.61	0.041	2.329	20.002	2.001	24.984	73.657
616	0.36	0.37	28.56	1.57	5.20	0.13	0.87	0.039	2.199	18.882	1.847	23.653	69.683
639	0.36	0.09	14.68	2.11	15.34	0.05	0.04	0.001	0.180	1.693	0.087	1.677	5.143
641	0.17	0.15	13.76	2.31	21.24	0.06	0.18	0.001	0.146	1.394	0.060	1.346	4.142
642	0.17	0.15	11.05	1.86	9.69	0.05	0.56	0.000	0.052	0.517	0.002	0.456	1.425
662	0.26	0.26	6.45	1.95	11.45	0.04	0.02	0.000	0.006	0.067	0.002	0.046	0.149
673	0.31	0.32	8.51	1.71	7.13	0.06	0.04	0.000	0.017	0.178	0.003	0.140	0.445
683	0.15	0.13	7.57	1.83	9.17	0.04	0.50	0.000	0.011	0.119	0.003	0.088	0.284
687	0.26	0.25	16.38	1.83	9.13	0.08	0.53	0.002	0.256	2.363	0.145	2.440	7.443
700	0.30	0.30	8.12	2.32	21.61	0.05	0.01	0.000	0.017	0.181	0.004	0.140	0.445
707	0.17	0.14	8.50	2.08	14.49	0.04	0.25	0.000	0.019	0.201	0.003	0.159	0.504
721	0.23	0.22	10.51	1.84	9.30	0.06	0.27	0.000	0.042	0.423	0.000	0.365	1.144
736	0.47	0.50	28.05	2.25	19.23	0.14	0.11	0.045	2.581	22.182	2.215	27.641	81.526
743	0.20	0.18	11.87	2.16	16.68	0.06	0.26	0.000	0.077	0.752	0.017	0.682	2.124
749	0.20	0.18	25.85	2.35	22.79	0.10	0.10	0.031	1.913	16.499	1.533	20.158	59.683
754	0.32	0.32	55.69	2.33	22.06	0.20	0.08	0.943	41.454	353.715	45.827	519.766	1470.528
761	0.20	0.18	6.06	2.04	13.40	0.04	0.06	0.000	0.005	0.054	0.002	0.036	0.117
764	0.18	0.16	26.26	1.93	10.98	0.09	0.34	0.030	1.791	15.425	1.468	18.884	56.033
765	0.46	0.48	20.14	2.25	19.33	0.11	0.05	0.009	0.677	5.928	0.467	6.754	20.313
767	0.34	0.35	9.50	1.91	10.57	0.06	0.03	0.000	0.028	0.293	0.000	0.242	0.764
777	0.31	0.32	17.96	1.86	9.73	0.09	0.38	0.004	0.377	3.359	0.231	3.663	11.087
783	0.19	0.19	6.20	2.29	20.41	0.04	0.06	0.000	0.005	0.063	0.002	0.043	0.140
784	0.20	0.18	8.10	2.13	15.85	0.04	0.14	0.000	0.016	0.170	0.004	0.130	0.417
787	0.28	0.27	9.64	2.38	23.51	0.06	0.03	0.000	0.035	0.357	0.000	0.298	0.936
788	0.21	0.06	9.85	2.35	22.44	0.04	0.06	0.000	0.038	0.385	0.000	0.324	1.020
797	0.28	0.28	8.45	1.86	9.69	0.05	0.07	0.000	0.017	0.183	0.003	0.144	0.458
836	0.27	0.27	13.84	2.25	19.42	0.07	0.13	0.001	0.147	1.403	0.063	1.354	4.182
849	0.19	0.16	11.00	2.39	23.91	0.05	0.09	0.000	0.060	0.596	0.000	0.524	1.644
850	0.36	0.38	9.69	2.36	22.86	0.06	0.01	0.000	0.035	0.362	0.000	0.302	0.952
862	0.25	0.24	9.31	1.26	2.34	0.05	0.20	0.000	0.020	0.207	0.000	0.169	0.536
883	0.45	0.47	18.87	1.88	9.92	0.11	0.10	0.006	0.462	4.075	0.297	4.538	13.699
888	0.50	0.53	19.03	2.34	22.20	0.11	0.01	0.007	0.552	4.860	0.359	5.433	16.391
889	0.24	0.23	11.72	2.20	17.75	0.06	0.15	0.000	0.073	0.724	0.013	0.654	2.037
922	0.12	0.09	4.39	1.40	3.37	0.02	0.73	0.000	0.001	0.012	0.001	0.007	0.023

Table 3 (con't)

ID	R_* (R_\odot)	M_* (M_\odot)	P_{orb} (d)	R_p (R_\oplus)	M_p (M_\oplus)	a (AU)	HITE	T_{CPL}^{short} (Myr)	T_{CPL}^\oplus (Myr)	T_{CPL}^{long} (Myr)	T_{CTL}^{short} (Myr)	T_{CTL}^\oplus (Myr)	T_{CTL}^{long} (Myr)
939	0.21	0.19	15.47	2.49	27.81	0.07	0.01	0.002	0.248	2.308	0.128	2.329	7.128
941	0.34	0.35	14.37	2.35	22.72	0.08	0.05	0.001	0.177	1.671	0.083	1.636	5.042
943	0.34	0.35	15.75	2.45	26.37	0.09	0.02	0.002	0.264	2.451	0.141	2.493	7.619
960	0.31	0.31	19.38	2.03	13.18	0.10	0.33	0.007	0.541	4.756	0.361	5.354	16.135
986	0.19	0.17	19.35	2.34	22.34	0.08	0.13	0.007	0.591	5.192	0.396	5.824	17.616
991	0.16	0.14	18.71	1.74	7.49	0.07	0.49	0.005	0.424	3.746	0.282	4.160	12.568
992	0.22	0.21	23.10	1.53	4.71	0.09	0.82	0.014	0.918	7.955	0.699	9.417	28.126
1004	0.33	0.34	12.93	2.46	26.65	0.08	0.01	0.001	0.118	1.139	0.042	1.071	3.318
1005	0.22	0.21	6.66	2.12	15.47	0.04	0.05	0.000	0.007	0.079	0.003	0.056	0.180
1006	0.16	0.14	10.58	1.84	9.31	0.05	0.59	0.000	0.043	0.434	0.000	0.375	1.178
1011	0.22	0.21	9.00	2.25	19.39	0.05	0.08	0.000	0.025	0.264	0.001	0.213	0.675
1017	0.16	0.13	14.41	2.23	18.68	0.06	0.23	0.001	0.173	1.631	0.080	1.604	4.924
1026	0.21	0.20	20.09	1.59	5.40	0.08	0.83	0.007	0.534	4.679	0.372	5.310	16.026
1045	0.15	0.13	4.95	1.88	10.09	0.03	0.19	0.000	0.002	0.023	0.001	0.014	0.047
1048	0.29	0.30	20.06	2.24	19.08	0.10	0.22	0.009	0.665	5.826	0.466	6.611	19.902
1061	0.28	0.29	18.83	2.30	21.04	0.09	0.17	0.006	0.524	4.617	0.339	5.146	15.532
1063	0.36	0.37	18.42	2.25	19.30	0.10	0.11	0.006	0.471	4.170	0.303	4.600	13.948
1065	0.18	0.16	6.78	1.03	1.12	0.04	0.24	0.000	0.005	0.053	0.002	0.038	0.122
1070	0.24	0.23	13.55	1.92	10.86	0.07	0.37	0.001	0.122	1.165	0.050	1.116	3.449
1074	0.18	0.14	6.15	2.33	21.99	0.03	0.04	0.000	0.005	0.062	0.002	0.042	0.137
1079	0.18	0.16	38.38	1.74	7.57	0.12	0.08	0.156	7.716	65.867	7.400	88.859	256.968
1080	0.19	0.17	7.04	1.85	9.39	0.04	0.17	0.000	0.008	0.090	0.003	0.065	0.210
1095	0.55	0.57	35.15	2.40	24.42	0.17	0.03	0.131	6.678	57.077	6.161	75.404	219.077
1096	0.33	0.34	9.36	2.21	18.22	0.06	0.02	0.000	0.029	0.304	0.000	0.250	0.788
1105	0.39	0.41	14.16	2.28	20.38	0.08	0.04	0.001	0.163	1.546	0.072	1.510	4.641
1108	0.39	0.42	17.59	2.41	24.72	0.10	0.03	0.004	0.409	3.713	0.247	3.945	11.994
1135	0.25	0.25	6.59	2.25	19.14	0.04	0.01	0.000	0.007	0.079	0.003	0.055	0.179
1141	0.22	0.20	10.86	1.87	9.82	0.06	0.32	0.000	0.048	0.484	0.000	0.424	1.330
1145	0.28	0.28	7.11	2.04	13.59	0.05	0.01	0.000	0.009	0.100	0.003	0.072	0.233
1151	0.17	0.15	19.45	2.38	23.83	0.08	0.09	0.008	0.610	5.367	0.401	6.034	18.190
1161	0.30	0.31	10.50	2.12	15.53	0.06	0.07	0.000	0.046	0.462	0.000	0.399	1.249
1193	0.28	0.28	18.49	2.02	12.90	0.09	0.38	0.005	0.446	3.944	0.282	4.362	13.180
1202	0.41	0.44	14.20	2.18	17.28	0.09	0.03	0.001	0.160	1.519	0.070	1.483	4.569
1206	0.31	0.31	8.76	1.26	2.34	0.06	0.04	0.000	0.015	0.164	0.001	0.131	0.414
1225	0.53	0.55	26.60	1.71	7.12	0.14	0.13	0.029	1.746	15.034	1.425	18.506	54.706
1227	0.32	0.33	9.06	2.40	24.27	0.06	0.01	0.000	0.027	0.283	0.000	0.229	0.725
1235	0.38	0.40	10.36	1.83	9.10	0.07	0.01	0.000	0.039	0.398	0.000	0.341	1.074
1238	0.33	0.35	25.51	1.50	4.36	0.12	0.95	0.022	1.352	11.655	1.088	14.161	42.083
1239	0.30	0.31	10.06	2.04	13.42	0.06	0.08	0.000	0.037	0.381	0.000	0.323	1.016
1244	0.16	0.14	7.16	1.82	8.93	0.04	0.28	0.000	0.008	0.095	0.003	0.069	0.222
1247	0.16	0.14	4.24	1.41	3.50	0.03	0.06	0.000	0.001	0.011	0.001	0.006	0.020
1248	0.24	0.23	7.07	1.31	2.65	0.04	0.08	0.000	0.006	0.073	0.002	0.053	0.170
1269	0.44	0.45	14.38	2.29	20.55	0.09	0.02	0.001	0.174	1.645	0.082	1.612	4.966
1274	0.24	0.23	10.65	1.94	11.32	0.06	0.21	0.000	0.046	0.461	0.000	0.400	1.256
1283	0.16	0.14	41.62	1.94	11.21	0.12	0.01	0.239	11.456	97.721	11.265	134.245	386.664
1292	0.25	0.24	14.27	1.52	4.61	0.07	0.60	0.001	0.129	1.223	0.059	1.199	3.682
1294	0.21	0.19	9.57	1.63	5.91	0.05	0.39	0.000	0.026	0.271	0.000	0.225	0.711
1296	0.17	0.15	11.56	1.92	10.86	0.05	0.55	0.000	0.064	0.629	0.010	0.566	1.762
1297	0.21	0.19	23.43	2.47	27.04	0.09	0.03	0.020	1.327	11.489	1.002	13.634	40.715
1299	0.23	0.21	22.51	1.91	10.69	0.09	0.51	0.014	0.956	8.301	0.706	9.749	29.169
1306	0.16	0.14	6.62	1.64	6.10	0.04	0.29	0.000	0.006	0.066	0.002	0.046	0.148
1308	0.25	0.24	16.46	1.49	4.29	0.08	0.76	0.002	0.228	2.102	0.126	2.173	6.648
1324	0.26	0.25	21.86	2.02	13.11	0.10	0.45	0.013	0.881	7.661	0.636	8.924	26.740

Table 3 (con't)

ID	R_* (R_\odot)	M_* (M_\odot)	P_{orb} (d)	R_p (R_\oplus)	M_p (M_\oplus)	a (AU)	HITE	T_{CPL}^{short} (Myr)	T_{CPL}^\oplus (Myr)	T_{CPL}^{long} (Myr)	T_{CTL}^{short} (Myr)	T_{CTL}^\oplus (Myr)	T_{CTL}^{long} (Myr)
1331	0.50	0.53	52.33	2.08	14.38	0.22	0.41	0.671	29.953	255.484	31.801	370.594	1051.350
1341	0.23	0.21	11.93	1.40	3.40	0.06	0.53	0.000	0.059	0.577	0.012	0.526	1.636
1348	0.36	0.38	12.53	2.12	15.45	0.08	0.06	0.000	0.094	0.915	0.027	0.850	2.638
1363	0.36	0.38	21.64	2.15	16.35	0.11	0.21	0.013	0.879	7.653	0.632	8.891	26.654
1364	0.10	0.09	6.59	2.03	13.25	0.03	0.44	0.000	0.006	0.074	0.003	0.052	0.168
1365	0.58	0.59	32.88	2.09	14.72	0.17	0.07	0.088	4.667	39.921	4.292	51.875	151.272
1366	0.39	0.41	10.71	2.31	21.21	0.07	0.01	0.000	0.052	0.527	0.000	0.459	1.436
1369	0.26	0.28	13.57	2.07	14.18	0.07	0.27	0.001	0.129	1.229	0.053	1.177	3.638
1399	0.36	0.37	18.52	1.94	11.27	0.10	0.25	0.005	0.438	3.874	0.289	4.285	12.950
1402	0.43	0.13	27.39	1.84	9.19	0.09	0.20	0.035	2.055	17.682	1.706	21.934	64.740
1411	0.41	0.44	14.93	2.24	18.98	0.09	0.03	0.002	0.200	1.877	0.102	1.867	5.740
1422	0.24	0.23	20.22	2.27	19.77	0.09	0.22	0.009	0.691	6.047	0.470	6.887	20.720
1424	0.32	0.32	9.22	2.10	15.08	0.06	0.04	0.000	0.027	0.277	0.000	0.226	0.715
1431	0.25	0.25	7.28	2.45	26.29	0.05	0.01	0.000	0.011	0.123	0.004	0.090	0.290
1436	0.38	0.39	15.01	1.77	8.07	0.09	0.14	0.001	0.176	1.646	0.087	1.643	5.035
1447	0.17	0.15	12.54	2.16	16.57	0.06	0.33	0.000	0.096	0.929	0.027	0.863	2.679
1448	0.23	0.21	6.19	1.64	6.03	0.04	0.06	0.000	0.004	0.051	0.002	0.034	0.112
1452	0.21	0.19	26.30	1.29	2.55	0.10	0.73	0.023	1.389	11.963	1.133	14.644	43.456
1474	0.17	0.15	4.43	1.75	7.79	0.03	0.05	0.000	0.001	0.015	0.001	0.008	0.028
1491	0.29	0.28	9.95	1.82	8.93	0.06	0.12	0.000	0.033	0.339	0.000	0.286	0.900
1504	0.31	0.32	19.60	2.41	24.65	0.10	0.07	0.008	0.634	5.560	0.423	6.276	18.909
1508	0.39	0.41	18.85	2.02	13.09	0.10	0.15	0.006	0.483	4.264	0.312	4.748	14.333
1512	0.36	0.38	11.16	2.16	16.68	0.07	0.03	0.000	0.059	0.592	0.004	0.524	1.637
1520	0.17	0.15	9.97	2.20	17.84	0.05	0.23	0.000	0.038	0.387	0.000	0.327	1.029
1525	0.28	0.28	10.33	2.30	20.87	0.06	0.05	0.000	0.045	0.456	0.000	0.392	1.227
1542	0.26	0.25	9.02	2.03	13.18	0.05	0.09	0.000	0.024	0.249	0.000	0.201	0.638
1544	0.36	0.37	26.40	1.80	8.55	0.12	0.58	0.029	1.749	15.067	1.410	18.501	54.727
1552	0.33	0.33	38.48	1.92	10.73	0.15	0.48	0.168	8.297	70.831	7.901	95.535	276.312
1558	0.14	0.12	5.71	1.97	11.92	0.03	0.21	0.000	0.003	0.042	0.002	0.027	0.089
1569	0.33	0.33	13.44	1.73	7.41	0.08	0.20	0.001	0.110	1.054	0.044	1.006	3.112
1576	0.28	0.29	7.57	1.37	3.14	0.05	0.03	0.000	0.009	0.098	0.003	0.073	0.234
1582	0.19	0.17	7.71	1.66	6.35	0.04	0.28	0.000	0.011	0.119	0.003	0.090	0.288
1628	0.24	0.23	11.39	2.33	21.92	0.06	0.08	0.000	0.068	0.673	0.007	0.601	1.873
1650	0.34	0.35	41.40	1.82	8.86	0.17	0.55	0.224	10.756	91.739	10.727	126.084	362.317
1656	0.31	0.31	9.66	1.88	10.04	0.06	0.07	0.000	0.030	0.310	0.000	0.258	0.814
1659	0.17	0.15	9.21	2.28	20.25	0.05	0.14	0.000	0.028	0.292	0.000	0.238	0.753
1661	0.18	0.16	6.45	1.89	10.15	0.04	0.15	0.000	0.006	0.065	0.002	0.045	0.146
1671	0.18	0.16	4.12	2.16	16.71	0.03	0.01	0.000	0.001	0.013	0.001	0.007	0.023
1678	0.39	0.41	16.30	1.91	10.55	0.09	0.13	0.002	0.258	2.377	0.141	2.447	7.489
1705	0.20	0.18	13.95	1.07	1.30	0.06	0.84	0.001	0.094	0.895	0.042	0.866	2.673
1708	0.36	0.37	21.66	2.08	14.54	0.11	0.27	0.012	0.864	7.523	0.619	8.738	26.199
1709	0.39	0.42	26.77	2.09	14.66	0.13	0.29	0.034	2.038	17.537	1.691	21.579	63.960
1721	0.46	0.48	33.31	2.22	18.28	0.16	0.18	0.098	5.111	43.715	4.676	56.916	166.275
1726	0.23	0.22	13.84	2.27	19.99	0.07	0.17	0.001	0.148	1.411	0.064	1.361	4.203
1730	0.28	0.28	7.30	2.39	23.91	0.05	0.01	0.000	0.011	0.122	0.004	0.090	0.287
1738	0.44	0.46	36.76	2.24	18.92	0.17	0.25	0.153	7.641	65.242	7.287	86.970	252.764
1744	0.39	0.40	13.85	2.17	16.82	0.08	0.05	0.001	0.144	1.372	0.062	1.324	4.088
1758	0.37	0.37	12.98	2.08	14.56	0.08	0.06	0.001	0.108	1.039	0.037	0.980	3.033
1759	0.34	0.35	9.59	1.86	9.73	0.06	0.04	0.000	0.029	0.299	0.000	0.248	0.783
1760	0.41	0.43	17.42	1.15	1.68	0.10	0.18	0.003	0.243	2.216	0.145	2.345	7.133
1764	0.34	0.35	20.96	2.40	24.24	0.11	0.08	0.011	0.829	7.231	0.588	8.332	25.013
1768	0.21	0.20	10.06	1.93	10.92	0.05	0.28	0.000	0.036	0.367	0.000	0.311	0.979
1769	0.39	0.41	27.33	2.48	27.49	0.13	0.02	0.042	2.477	21.305	2.070	26.344	78.009
1783	0.18	0.15	13.34	2.20	17.72	0.06	0.29	0.001	0.125	1.196	0.048	1.142	3.519

Table 3 (con't)

ID	R_* (R_\odot)	M_* (M_\odot)	P_{orb} (d)	R_p (R_\oplus)	M_p (M_\oplus)	a (AU)	HTE	T_{CPL}^{short} (Myr)	T_{CPL}^\oplus (Myr)	T_{CPL}^{long} (Myr)	T_{CTL}^{short} (Myr)	T_{CTL}^\oplus (Myr)	T_{CTL}^{long} (Myr)
1794	0.19	0.20	7.27	2.14	16.10	0.04	0.15	0.000	0.010	0.112	0.003	0.082	0.265
1798	0.32	0.32	20.37	2.45	26.25	0.10	0.04	0.010	0.749	6.549	0.518	7.482	22.494
1804	0.16	0.09	17.79	1.94	11.19	0.06	0.40	0.004	0.372	3.354	0.225	3.607	10.920
1809	0.18	0.16	9.96	2.44	26.13	0.05	0.04	0.000	0.040	0.413	0.000	0.349	1.099
1821	0.30	0.30	37.63	2.03	13.23	0.15	0.36	0.158	7.873	67.232	7.492	90.282	261.351
1832	0.24	0.23	6.28	2.06	13.93	0.04	0.03	0.000	0.005	0.062	0.002	0.042	0.138
1844	0.29	0.29	15.40	1.70	6.89	0.08	0.42	0.002	0.190	1.768	0.100	1.785	5.460
1849	0.34	0.35	19.07	2.41	24.87	0.10	0.05	0.007	0.568	5.003	0.367	5.589	16.866
1852	0.32	0.32	19.01	2.02	12.97	0.10	0.31	0.006	0.499	4.398	0.326	4.917	14.833
1866	0.17	0.15	15.30	1.77	8.02	0.06	0.67	0.002	0.190	1.771	0.097	1.782	5.453
1877	0.23	0.21	5.71	2.08	14.41	0.04	0.02	0.000	0.004	0.044	0.002	0.028	0.093
1878	0.14	0.14	9.96	1.08	1.32	0.05	0.94	0.000	0.024	0.242	0.000	0.204	0.644
1881	0.25	0.24	10.60	2.44	25.90	0.06	0.02	0.000	0.052	0.524	0.000	0.455	1.424
1887	0.46	0.48	20.36	2.19	17.45	0.11	0.06	0.009	0.695	6.078	0.481	6.944	20.876
1913	0.33	0.34	14.13	2.35	22.69	0.08	0.05	0.001	0.165	1.563	0.074	1.527	4.691
1919	0.12	0.10	9.41	1.40	3.41	0.04	0.78	0.000	0.022	0.231	0.000	0.190	0.600
1923	0.28	0.28	8.18	1.96	11.64	0.05	0.06	0.000	0.015	0.167	0.003	0.128	0.411
1941	0.21	0.22	6.23	1.96	11.64	0.04	0.10	0.000	0.005	0.058	0.002	0.040	0.129
1942	0.23	0.22	6.25	1.83	9.02	0.04	0.05	0.000	0.005	0.057	0.002	0.039	0.126
1945	0.25	0.24	7.62	1.75	7.66	0.05	0.08	0.000	0.011	0.118	0.003	0.088	0.283
1949	0.17	0.15	7.88	2.40	24.38	0.04	0.05	0.000	0.015	0.165	0.004	0.126	0.401
1950	0.17	0.14	4.52	1.96	11.70	0.03	0.05	0.000	0.001	0.017	0.001	0.010	0.033
1958	0.27	0.27	15.27	2.38	23.69	0.08	0.08	0.002	0.228	2.132	0.118	2.144	6.562
1963	0.23	0.21	12.84	1.89	10.29	0.06	0.40	0.000	0.097	0.936	0.033	0.880	2.717
1974	0.40	0.42	26.66	1.94	11.27	0.13	0.34	0.032	1.913	16.457	1.549	20.264	59.912
1975	0.25	0.26	6.94	2.24	19.11	0.05	0.03	0.000	0.009	0.097	0.003	0.069	0.223
1978	0.21	0.19	6.76	1.99	12.21	0.04	0.09	0.000	0.007	0.081	0.003	0.057	0.184